Adaptations for bipedal walking: Musculoskeletal structure and three-dimensional joint mechanics of humans and bipedal chimpanzees (*Pan troglodytes*)

Matthew C. O'Neill[a], Brigitte Demes[b], Nathan E. Thompson[c], Susan G. Larson[b], Jack T. Stern, Jr.[b], Brian R. Umberger[d]

[a] *Department of Anatomy, Midwestern University, Glendale, AZ 85308 USA*

[b] *Department of Anatomical Sciences, Stony Brook University School of Medicine, Stony Brook, NY 11794 USA*

[c] *Department of Anatomy, New York Institute of Technology College of Osteopathic Medicine, Old Westbury, NY 11568 USA*

[d] *School of Kinesiology, University of Michigan, Ann Arbor, MI 48109-2013 USA*

Corresponding author.

Email: moneill@midwestern.edu (M. C. O'Neill)

1 **Abstract**

2

3   Humans are unique among apes and other primates in the musculoskeletal design of their
4   lower back, pelvis and lower limbs. Here, we describe the three-dimensional ground
5   reaction forces and lower/hind limb joint mechanics of human and bipedal chimpanzee
6   walking over a full stride and test whether: 1) the estimated limb joint work and power
7   during stance phase, especially the single-support period, is lower in humans than bipedal
8   chimpanzees, 2) the limb joint work and power required for limb swing is lower in
9   humans than in bipedal chimpanzees, and 3) the estimated total mechanical power during
10   walking, accounting for the storage of passive elastic strain energy in humans, is lower in
11   humans than in bipedal chimpanzees. Humans and bipedal chimpanzees were compared
12   at matched dimensionless and dimensional velocities. Our results indicate that humans
13   walk with significantly less work and power output in the first double-support period and
14   the single-support period of stance, but markedly exceed chimpanzees in the second-
15   double support period (i.e., push-off). Humans generate less work and power in limb
16   swing, although the species difference in limb swing power was not statistically
17   significant. We estimated that total mechanical positive 'muscle fiber' work and power
18   were 46.9% and 35.8% lower, respectively, in humans than bipedal chimpanzees at
19   matched dimensionless speeds. This is due in part to mechanisms for the storage and
20   release of elastic energy at the ankle and hip in humans. Further, these results indicate
21   distinct heel strike and lateral balance mechanics in humans and bipedal chimpanzees,
22   and suggest a greater dissipation of mechanical energy through soft tissue deformations
23   in humans. Together, our results document important differences between human and
24   bipedal chimpanzee walking mechanics over a full stride, permitting a more
25   comprehensive understanding of the mechanics and energetics of chimpanzee bipedalism
26   and the evolution of hominin walking.

27

28   ***Keywords:*** Force; Work; Power; Elastic Energy; Bipedalism; Locomotion

1. Introduction

As humans, we are unique among apes and other primates in the musculoskeletal design of our lumbar column, pelvis and lower limbs. In particular, we possess a mobile lower back, a short pelvis and long lower limbs with short feet. This is distinct from the relatively immobile lumbar column, tall pelvis and short hind limbs with long feet characteristic of living African apes (e.g., Schultz, 1930, 1961; Ward, 1993; Pilbeam and Lieberman, 2017). Our limb muscle masses are more proximally located and are made up of relatively short muscle fibers and long distal limb tendons as compared to African apes (e.g., Thorpe et al., 1999; O'Neill et al., 2013, 2017). Among other capabilities, these traits are thought to facilitate humans walking with a stable pelvis on adducted, extended lower limbs (O'Neill et al., 2015), using as much as 75% less energy per distance walked than a bipedal chimpanzee (Rodman and McHenry, 1980; Sockol et al. 2007). Understanding when and where in a full stride lower/hind limb mechanics differ between human and bipedal chimpanzee walking is important for elucidating how our interspecific differences in musculoskeletal structure affect joint loading, muscle-tendon behavior and the metabolic cost of walking.

Over a walking stride, humans generate a coordinated sequence of three-dimensional (3-D) moments and power that with some exceptions, are minimal near the middle single-support period and contribute to a burst in positive power during the second double-support period (i.e., push-off), with significant moments and power continuing throughout limb swing. At the hip, in particular, there are substantial non-sagittal plane moments, work and power over a stride (e.g., Eng and Winter, 1995), comprehensive measurements of which are needed for accurate determination of skeletal loading (e.g., Stansfield et al., 2003), muscle-tendon force and fascicle length change (e.g., Arnold and Delp, 2011). Across the limb, the instantaneous 3-D joint moments, work and power reflect the net contributions from active muscle-tendon units and passive, soft tissues at each joint throughout the full gait cycle. While it is difficult to decompose the individual contributions of a mobile lower back, a short pelvis, and long lower limbs and short feet via joint-level analyses alone, these traits can be expected to act together to reduce the total mechanical work and power output of an erect human walking stride when compared to facultative bipeds, such as bipedal chimpanzees.

1   In addition to our skeletal structure, our more proximal limb segment masses and
2   long, thin distal limb tendons can be expected to further reduce the total mechanical work
3   and power output in a walking stride. It has long been hypothesized that more proximal
4   lower limb-mass distribution reduces the moment of inertia, and therefore the mechanical
5   power required for limb swing (e.g., Gray, 1968; Hildebrand, 1985), including in fossil
6   hominins (Jungers and Stern, 1988). Human limb mass perturbations provide some
7   support for this view, demonstrating that a distal shift of the mass-specific moment of
8   inertia increases the limb swing mechanical power and metabolic costs of walking (Royer
9   and Martin, 2005; Browning et al., 2007). Still, the magnitude of these perturbations was
10   large, and the resulting changes in limb segment inertial properties can exceed the
11   difference between humans and African apes or some Old World monkeys (e.g., Isler et
12   al., 2006; Supplementary Online Material [SOM] Table S1).

13   Long, thin tendons, as well as other soft tissues (e.g., ligaments, aponeuroses), have a
14   significant capacity for passive elastic strain and reducing the mechanical work and
15   power required of muscle fibers (e.g., Alexander, 1988; Roberts, 2016). While often
16   associated with bouncing gaits, the storage and release of elastic strain energy in human
17   walking is now well established. Direct measurements of ankle plantar flexor muscle-
18   tendon behavior have shown that the Achilles tendon is stretched during single-support
19   period and then recoils in the second double-support period, making a substantial
20   contribution to positive ankle power at push-off (e.g., Fukunaga et al., 2001; Ishikawa et
21   al., 2005). However, elastic mechanisms in human walking are not limited to the ankle.
22   The hip joint produces a large component of the total limb mechanical work and power
23   output in walking (e.g., Eng and Winter, 1995; Farris and Sawicki, 2012a; Schache et al.,
24   2015), and a portion of this is derived from non-muscular tissues stretched during the
25   single-support period, including hip joint ligaments, associated tissues and aponeuroses
26   (e.g., Whittington et al., 2008; Eng et al., 2015). Although there is extensive quantitative
27   data on human walking, little comparative data exist that permit a direct assessment of
28   whether these presumed musculoskeletal adaptations interact to reduce the total
29   mechanical work and power output as compared to a biped that lacks this lower back,
30   pelvis and lower limb structure, such as bipedal chimpanzees. Indeed, the absence of
31   comprehensive, speed-controlled comparisons has left the unique aspects of human

1 walking mechanics still not well defined, despite their critical significance for
2 interpreting skeletal trait evolution in hominins.

3   This is not to suggest that data on bipedal chimpanzee walking mechanics are
4 unknown. A seminal series of lab-based studies provided the first quantitative
5 comparison of human and bipedal chimpanzee walking mechanics in the 1970s and
6 1980s (i.e., Yamazaki et al., 1979; Okada, 1985; Yamazaki, 1985). These studies include
7 important, initial insights into the ground forces and joint moments of human and
8 facultative bipedal walking in chimpanzees and other taxa; however, the experimental
9 design (i.e., mismatched speeds, markerless joint kinematics) as well as the absence of
10 variance metrics permits only limited interspecific inferences. Indeed, forces and
11 moments are velocity-dependent parameters (e.g., Farris and Sawicki, 2012a; Schache et
12 al., 2015; see also SOM) and, as such, interspecific comparisons are well known to be
13 sensitive to speed. More careful, speed-controlled comparisons of human and bipedal
14 chimpanzee walking have examined two-dimensional (2-D) sagittal plane stance phase
15 joint moments (Sockol et al. 2007; see also Pontzer et al., 2009), but exclude joint work
16 and power as well as limb swing. Thus, a comprehensive characterization of the 3-D
17 moments, work and power of human and bipedal chimpanzee walking over a full stride is
18 still unavailable.

19   Here, we evaluate how human and bipedal chimpanzee musculoskeletal structure
20 affects their 3-D moments, work, and power output. Specifically, we provide the first
21 comprehensive description and direct, speed-controlled comparisons of stride-to-stride
22 and intraspecific variation of human and bipedal chimpanzee ground reaction forces, as
23 well as the lower/hind limb joint moment and power profiles of each species over a full
24 walking stride. Based on their differences in musculoskeletal structure, we then test
25 whether: 1) the estimated limb joint work and power during stance phase, especially the
26 single-support period, is lower in humans than bipedal chimpanzees, 2) the limb joint
27 work and power required for limb swing is lower in humans than in bipedal chimpanzees,
28 and 3) the estimated total mechanical power during walking, accounting for the storage of
29 passive elastic strain energy in humans, is lower in humans than in bipedal chimpanzees.
30 For completeness, the 3-D mechanics of bipedal chimpanzees and humans were
31 compared at matched dimensionless (i.e., relative-speed match) and dimensional (i.e.,

4

1   absolute-speed match) speeds. Matched dimensionless speed comparisons minimize the

2   effects due to differences in body size or walking speed, while emphasizing those arising

3   specifically from differences in musculoskeletal design between humans and

4   chimpanzees. The dimensional comparison, in contrast, permits an assessment of how

5   sensitive the interspecific differences in 3-D mechanics are to walking speed.

6

7   **2.   Materials and methods**

8   *2.1. Human and chimpanzee subjects*

9   Three-dimensional kinematic and ground force data were collected for three humans

10 (*Homo sapiens*: age = 24.3 ± 2.3 years, mass = M_b: 79.2 ± 6.2 kg) and three chimpanzees

11 (*Pan troglodytes*: age = 5.5 ± 0.2 years, mass = M_b: 26.5 ± 6.7 kg) during bipedal

12 walking. All subjects were male. Bipedal chimpanzees walked across an 11 m rigid, level

13 runway at self-selected speeds, following an animal trainer offering a food reward.

14 Human data were then collected during walking along a 20 m rigid, level runway at

15 speeds matching the chimpanzee dataset in dimensionless (i.e., relative-speed match) and

16 dimensional (i.e., absolute-speed match) forms (Fig. 1; Table 1; SOM Table S2) using an

17 instantaneous speed. Bipedal chimpanzees were trained for 1 hour d^{-1}, 3–5 days wk^{-1}, for

18 at least six months prior to the start of data collection. The University of Massachusetts

19 Amherst Institutional Research Board and the Stony Brook University Institutional

20 Animal Care and Use Committee approved all human (SPHHS-HSRC-13-36) and

21 chimpanzee (2009-1731-FAR-USDA) experiments, respectively. Prior to data collection,

22 the human subjects each provided written informed consent.

23

24 *2.2. Three-dimensional marker and ground reaction force data*

25   The procedures used for marker data collection and 3-D joint kinematic

26 measurements in humans and chimpanzees have been detailed in O'Neill et al. (2015). In

27 brief, marker positions were recorded using synchronized high-speed video cameras.

28 Marker data for the humans were collected using an eleven-camera system recording at

29 240 Hz (Qualisys, Inc.; Gothenburg), while chimpanzee data were collected using a four-

30 camera system recording at 150 Hz (Xcitex, Inc., Woburn). The calibrated video

31 recording volume for the humans was created using a wand-based nonlinear

1 transformation approach, while the recording volume for the chimpanzees was

2 established using direct linear transformation and a custom-built calibration frame.

3 Marker locations were digitized using Qualisys Track Manager software (Qualisys, Inc.;

4 Gothenburg) for the humans and ProAnalyst software (Xcitex, Inc., Woburn) for the

5 chimpanzees.

6   Ground reaction forces were collected using floor-mounted force platforms set into

7 the runway flush to its surface, within the calibrated video recording volume. Two force

8 platforms (AMTI, Watertown) sampling at 2400 Hz were used to record individual limb

9 forces from humans, whereas an array of four force platforms (AMTI, Watertown)

10 sampling at 1500 Hz were used to collect individual limb forces in chimpanzees

11 throughout a bipedal walking stride. Marker data and force platform data were collected

12 using a manual trigger that started and stopped video and force platform recording

13 simultaneously. The x-, y-, and z- force data were low pass filtered with a cut-off

14 frequency set to 60 Hz, while the marker data were filtered at 4–6 Hz. The force data

15 were then downsampled to 240 or 150 Hz to match the synchronous video data for each

16 species using MATLAB v. R2015 (The Mathworks, Inc., Natick). The x-, y-, and z- data

17 from each force platform was transformed into the marker global coordinate system using

18 markers positioned on the corner of each platform during the calibration of the video

19 recording volume, prior to the start of an experiment. This permitted spatial

20 transformations between the global coordinate system and the local force plate coordinate

21 systems.

22

23 *2.3. Musculoskeletal models and inverse dynamics*

24   Three-dimensional kinematics and ground force data were processed using generic

25 musculoskeletal models of the pelvis and lower/hind limbs of an adult human (Delp et al.,

26 1990) and an adult chimpanzee (O'Neill et al., 2013) scaled to the size of each subject

27 using anatomical segment markers (O'Neill et al., 2015). All models included skeletal

28 geometry of the pelvis and lower/hind limbs relevant to determining 3-D mechanics of

29 the hip, knee, and ankle (talocrual) joints.

30   An inverse kinematics algorithm was used to determine the 3-D coordinates of the

31 scaled model of each subject of each species over the full gait cycle (O'Neill et al., 2015).

1   This was done through a least-squares minimization of the discrepancy between the

2   experimentally determined marker positions and the corresponding marker positions on

3   the scaled model, subject to constraints enforced by the anatomical models of the joints

4   (Lu and O'Connor, 1999; Delp et al., 2007). The 3-D kinematics and force data were

5   combined with the scaled musculoskeletal model of each subject and used to calculate the

6   net joint moments and mechanical power associated with the joint moments. Inverse

7   dynamics combines rigid-segment linear and rotational motion, ground reaction forces,

8   and limb segment inertial parameters to calculate net forces and moments at each joint.

9   Detailed limb segment inertial parameters are provided for the adult human and adult

10   chimpanzee models in the supplemental materials (SOM Table S1). These generic

11   parameters were scaled to the size of each subject based on subject-specific

12   measurements of body mass and segment lengths.

13   The instantaneous joint powers were computed at the jth joint over both the stance and

14   swing phase of walking as the dot product of the jth joint moment and joint angular

15   velocity vectors. Because the joint angles and joint moments were both expressed in the

16   anatomically relevant but non-orthogonal joint reference frames, the moment and angular

17   velocity vectors were both transformed into a common orthogonal reference frame before

18   computing the dot product. This transformation is especially critical when the segments

19   forming a joint are not closely aligned with the global reference frame, as in the

20   abducted, flexed-limb walking of bipedal chimpanzees (O'Neill et al., 2015). The hip,

21   knee, and ankle powers were then multiplied by two to represent the work done by both

22   limbs over a full stride:

23

24
$$W_j^+ = 2 \cdot \int_{t_1}^{t_2} P_j^+ dt \qquad\qquad (1)$$

25
$$W_j^- = 2 \cdot \int_{t_1}^{t_2} P_j^- dt \qquad\qquad (2)$$

26

27   The positive and negative mechanical work of the jth joint was computed by integrating

28   over the time duration t_1 to t_2 of a walking stride, where t_1 and t_2 are the start and end of

29   the first double-support period (ds1), single-support period (ss), second-double support

1   period (ds2) of stance phase or the limb swing phase (sw). The total limb positive and

2   negative work in the ith period or phase of a stride were calculated as the sum of the

3   positive and negative work at each of the n joints ($n = 3$ for each species):

4

5
$$W_i^+ = \sum_{j=1}^{N} W_j^+ dt \qquad\qquad (3)$$

6
$$W_i^- = \sum_{j=1}^{N} W_j^- dt \qquad\qquad (4)$$

7

8   Total positive and negative mechanical work for the complete stride (W_{tot}^+, W_{tot}^-) were

9   calculated as the sum of the positive or negative work for the first double-support period

10 (W_{ds1}^+; W_{ds1}^-), single-support period (W_{ss}^+; W_{ss}^-), second double-support period (W_{ds2}^+; W_{ds2}^-

11) and limb swing (W_{sw}^+; W_{sw}^-). The positive and negative work terms were

12 subsequently divided by the stride time to determine average power output (P_i^+; P_i^-).

13

14 *2.4. Elastic and 'muscle fiber' work and power estimates*

15   In human walking, passive elastic energy is stored at the ankle and hip joints during

16 the single-support period and released in the second-double-support period as well as,

17 perhaps, in early limb swing (e.g., Fukunaga et al., 2001; Ishikawa et al., 2005;

18 Whittington et al., 2008; Eng et al., 2015). The structures most responsible for this are the

19 Achilles tendon at the ankle and the joint capsule ligaments and iliotibial tract at the hip.

20 A similar mechanism is not expected at the knee joint due to the opposite phasing (i.e.,

21 positive power in single-support and negative power in the second-double-support

22 period) of the joint power during late stance phase. We estimated that elastic energy was

23 stored during the portion of the single-support period in which the relevant joint power

24 curve was negative. We assumed that the elastic energy storage equaled the negative

25 work, and that all of the elastic energy stored was supplied to the subsequent period of

26 positive power generation. At both the dimensionless and dimensional walking speeds,

27 the positive power generation occurred during the double-support period for the ankle, or

28 the double-support period and early limb swing for the hip. As such, the net positive

29 elastic work during the single-support period was estimated as:

8

1

$$W_{el,j} = 2 \cdot \left| \int_{t_{ss_1}}^{t_{ss_2}} P_j^- \, dt \right|$$

2   (5)

3

4   where $W_{el,j}$ is the elastic work absorbed at the jth joint (a: ankle; h: hip) during the single-

5   support period of the stance phase of a walking stride, and used to generate positive

6   elastic recoil. The positive elastic power output was computed by dividing the positive

7   elastic work by stride time. Therefore, the total 'muscle fiber' work and power were the

8   estimated positive elastic work at the ankle ($W_{el,a}$) and hip ($W_{el,h}$) subtracted from the total

9   positive mechanical work (W^+_{tot}). The positive mechanical power attributable to 'muscle

10   fiber' was computed by dividing the 'muscle fiber' work by stride time.

11

12   *2.5. Analysis and statistics*

13   Four strides per subject were analyzed for the humans (H) and chimpanzees (C). All

14   3-D moment and power data were normalized to 101 points over one full stride,

15   facilitating comparisons of multiple strides. This also permitted the mean ± standard

16   deviation (s.d.) of the moment and power curves to be determined per species.

17   For the chimpanzees, walking speed was calculated as the average of the

18   instantaneous forward velocity of four markers (i.e., 3 pelvis, 1 hip marker) over the full

19   stride, while for humans a marker placed over the sacrum was used. To account for

20   differences in body size among subjects and species, analyses were performed with

21   dimensionless variables, using the base units of body mass M_b, gravitational acceleration

22   g, and average lower/hind limb length L. Lower/hind limb length was measured as the

23   average height of the greater trochanter marker from the ground during quiet standing for

24   humans and during the middle of the single-support period for chimpanzees (H = 0.92 ±

25   0.05, C = 0.39 ± 0.02 m). Velocity (v) was made dimensionless by the divisor $(gL)^{0.5}$ and

26   as the Froude number ($Fr = v^2/gL$). Force was made dimensionless by the divisor $M_b g$,

27   moment and work by $M_b gL$ and power by $M_b^{1.5} g^{1.5} L^{0.5}$. In all cases, stance, swing, and

28   stride duration were determined based on the ground reaction forces.

29   To compare the stride-to-stride, intraspecific, and interspecific variation of the ground

30   reaction forces of our human and chimpanzee samples, the adjusted coefficient of

1 multiple correlation (CMC) was used (Kadaba et al. 1989, r^2_a). The CMC represents the

2 correlation of the ground reaction force among strides for each individual (i.e., stride-to-

3 stride variation) or among the individuals (i.e., intraspecific variation). The balanced

4 human and chimpanzee datasets permit a direct, interspecific comparison of CMCs

5 computed using the species means.

6   To compute the difference in dimensionless work and power between humans and

7 bipedal chimpanzees, the percent difference was calculated as $|(s_1 - s_2)|/[(s_1 + s_2)/2] \cdot 100$,

8 where s_1 (species 1) and s_2 (species 2) are the species mean work and power parameters.

9 Because the sample was balanced, a two-level nested analysis of variance (ANOVA) was

10 used to compare work and power output in each period or phase of a walking stride (i.e.,

11 double-support 1, single support, double-support 2, limb swing; Fig. 1), as well as the

12 total mechanical work and power output over a full stride to test hypotheses 1-3. A two-

13 level nested approach allowed repeated individual subject trials to be incorporated as

14 random effects and was therefore preferred to an independent samples t-test based on

15 subject means. Statistical significance was set at $\alpha = 0.05$. The nested ANOVA was

16 computed in R v. 4.0.2 using the base package for Mac OS (R Development Core Team,

17 2020).

18   Due to the small sample sizes for each species, omega-squared (ω^2) was also used to

19 assess the effect size of the difference between chimpanzees and human comparisons

20 outlined in hypotheses 1-3. Effect size descriptive thresholds were $\omega^2 \leq 0.01$ = 'small',

21 $\omega^2 \leq 0.06$ = 'medium', $\omega^2 \leq 0.14$ = 'large' (Field, 2013). Effect size calculations were

22 implemented in R v. 4.0.2 using the 'effectsize' package (R Development Core Team,

23 2020).

24

25 **3. Results**

26   The average walking speeds of humans and chimpanzees were 1.66 ± 0.06 and $1.09 \pm$

27 0.10 m s^{-1}, respectively. These correspond to similar dimensionless velocities (v'; H =

28 0.56 ± 0.01, C = 0.56 ± 0.06) and Fr numbers (H = 0.31 ± 0.02, C = 0.31 ± 0.06) (Table

29 1). These speeds are close to—but a bit faster than—the preferred overground speeds for

30 human walking, and well below the expected walk-run transition speed for terrestrial

31 mammals (i.e., $v' = 0.7$; $Fr = 0.5$; Alexander, 1989; Kram et al., 1997).

1   Here, we describe the three-dimensional ground reaction forces, lower/hind limb joint

2   moment and power profiles of humans and bipedal chimpanzees walking over a full

3   stride at matched dimensionless speeds. The limb-joint work and power in stance, swing

4   and over a full stride are determined to test hypotheses 1-3.

5

6   *3.1. Ground reaction forces, stride-to-stride, and intraspecific variation*

7   The ground reaction forces of humans and chimpanzees were different in both

8   magnitude and pattern (Fig. 2). The vertical force was monophasic in bipedal

9   chimpanzees, lacking the second peak from the single-support period into the second

10   double-support period that is characteristic of human walking. The bipedal chimpanzee

11   anterior-posterior force was distinct from humans, as it exhibited a smaller peak force in

12   both posterior and anterior directions, while the mediolateral force was larger, most

13   notably during the single-support period.

14   The CMCs were smaller between strides than between individuals for both humans

15   and bipedal chimpanzees (Table 2). This indicates that there is more variation among

16   humans and chimpanzees in ground reaction forces than there is within a given individual

17   from one stride to the next. Among individuals, the medio-lateral force was the most

18   variable in chimpanzees ($r^2_a = 0.847 \pm 0.012$) and humans ($r^2_a = 0.916 \pm 0.038$). Directly

19   comparing the CMC values of human and chimpanzee samples indicates that, on average,

20   chimpanzees are more variable in their ground reaction force stride-to-stride than humans

21   at matched dimensionless speeds (H = $r^2_a = 0.985$, C = $r^2_a = 0.922$).

22

23   *3.2. Limb-joint moment profiles*

24   As expected, humans and chimpanzees were quite different in the magnitude and

25   pattern of the limb joint moments over a full stride (Fig. 3; Table 3). At the hip,

26   chimpanzees exhibit the largest joint moments in hip flexion-extension, with peak hip

27   extension moment occurring in the first double-support period and continuing throughout

28   the single-support period of stance. Unlike humans, for whom the net flexion moment

29   begins near midstance, the net flexion moment does not occur until the second-double

30   support period in bipedal chimpanzee walking. Humans and chimpanzees were opposite

31   in phase in the frontal plane, where chimpanzees exhibit a net hip adduction moment

1   throughout stance that peaks in the second-double support period. Near the middle of the

2   single support period, the hip adduction-abduction moment approaches zero in both taxa.

3   Chimpanzees exhibit substantial hip rotational moments, with a large internal rotation

4   moment throughout the single-support and second double-support periods. During limb

5   swing, chimpanzees exceed humans in the magnitude of internal and external rotational

6   moments.

7   Humans and chimpanzees both exhibit an initial knee flexion moment in the first

8   double-support period, and then rapidly shift to a large net extension moment at the start

9   of the single-support period. Unlike humans, chimpanzees have a net knee extension

10   moment throughout the single and second double-support periods. The pattern and

11   magnitude of knee flexion-extension moments in limb swing are similar for both species.

12   The chimpanzee exhibits a net ankle plantar flexion moment throughout stance phase,

13   including during the first double-support period. This differs from humans, who exhibit a

14   net dorsiflexion moment in the first double-support period, likely associated with our

15   distinct 'heel strike'. Whereas chimpanzees maintain a near-constant ankle plantar

16   flexion moment throughout the remainder of stance, there is an increase in the magnitude

17   of the net plantar flexion moment throughout the single and second double-support

18   periods in humans, which peaks in the second-double support period. For both species,

19   there is a small net dorsiflexion moment throughout limb swing, on average.

20

21   *3.3. Limb-joint power profiles*

22   The magnitude as well as pattern of joint powers differed between humans and

23   bipedal chimpanzees (Fig. 4; Table 4). In both humans and chimpanzees, there was

24   negative hip power in the first double-support period. In the single-support period, there

25   is an initial period of hip energy generation followed by hip energy absorption in humans,

26   whereas chimpanzee hips generate energy throughout this period. In the second-double

27   support period, there was positive power in human hips, whereas there was negative

28   power in chimpanzee hips. For humans, the second double-support period positive power

29   continues into limb swing, ending with a small burst of energy absorption. Chimpanzees

30   generate substantial positive hip power in the first half of limb swing, ending with a small

31   burst of energy generation.

12

1   At the knee joint, there was a substantial positive power peak in the first double-

2   support period in both chimpanzees and humans, followed by complex, cyclical pattern

3   of energy absorption and generation through the single-support and second double-

4   support periods. In the middle of the single-support period, chimpanzees have a small

5   burst of energy generation, whereas humans are near zero power output. Throughout limb

6   swing, there was substantial negative power at the knee in both species, especially in the

7   second half of swing phase.

8   The ankle joint in chimpanzees is characterized by energy absorption followed by

9   energy generation over the stance phase. This is distinct from humans, where a small

10   amount of energy absorption occurs in the first double-support period, followed by a

11   period of negative power at the end of the single-support period and then substantial

12   positive power output in the second-double support period. The peak dimensionless

13   positive power in the second-double support period is almost three times greater in

14   humans than chimpanzees at matched dimensionless walking speeds, on average (Table

15   4). For both species, there is a relatively small amount of energy generation from the

16   ankle throughout limb swing.

17

18   *3.4. Limb-joint work and power in stance (hypothesis 1)*

19   Humans generate less dimensionless positive mechanical work (W^+_{ds1}: $F_{1,18} = 21.38$, p

20    $= 0.0099$; $\omega^2 = 0.77$) and power (P^+_{ds1}: $F_{1,18} = 12.67$, $p = 0.0236$; $\omega^2 = 0.66$) than

21   chimpanzees during the first double-support. The same was true for the single-support

22   period positive mechanical work (W^+_{ss}: $F_{1,18} = 27.58$, $p = 0.0063$; $\omega^2 = 0.82$) and power

23   (P^+_{ss}: $F_{1,18} = 13.51$, $p = 0.0213$; $\omega^2 = 0.68$). In the second double-support period, humans

24   generate much more positive mechanical work (W^+_{ds2}: $F_{1,18} = 38.15$, $p = 0.0035$; $\omega^2 =$

25   0.86) and power than chimpanzees (P^+_{ds2}: $F_{1,18} = 76.51$, $p = 0.0009$ $\omega^2 = 0.93$; Fig. 5). In

26   all cases, the effect sizes were 'large'. This provides partial support for our first

27   hypothesis.

28

29   *3.5. Limb-joint work and power in swing (hypothesis 2)*

30   Humans generate less dimensionless positive mechanical work (W^+_{sw}: $F_{1,18} = 16.71$, p

31    $= 0.0016$; $\omega^2 = 0.72$) and power (P^+_{sw}: $F_{1,18} = 6.649$, $p = 0.0614$; $\omega^2 = 0.48$) than

1   chimpanzees in limb swing. The difference in positive work was significant, but the

2   difference in power only near significant; however, in both cases the effect size was

3   'large' (Fig. 6). This provides partial support for our second hypothesis.

4

5   *3.6. Total mechanical work and power (hypothesis 3)*

6   The total dimensionless positive mechanical work (W^+_{tot}) and power (P^+_{tot}) was

7   23.3% and 12.0% smaller in humans than chimpanzees, respectively. The difference in

8   mechanical work was 'large' and significant ($F_{1,18} = 11.55$, $p = 0.0273$; $\omega^2 = 0.64$), while

9   the difference in power was a 'medium' effect, and not statistically significant ($F_{1,18} =$

10   1.372, $p = 0.3070$; $\omega^2 = 0.06$). The modest differential in total mechanical power is due to

11   the substantial positive power output in the second double-support period of a human

12   walking stride. However, when the mechanical work and power attributable to elastic

13   storage and release at the human ankle and hip were accounted for, the estimated total

14   positive 'muscle fiber' work and power percent differential between species increased to

15   46.9% and 35.8%, respectively. The differences in estimated total positive 'muscle fiber'

16   work ($F_{1,18} = 33.19$, $p = 0.0045$, $\omega^2 = 0.84$) and power ($F_{1,18} = 10.56$, $p = 0.0314$, $\omega^2 =$

17   0.61) between species were both significant, and the effect sizes were 'large' (Fig. 7),

18   supporting our third hypothesis.

19

20   *3.7. Distribution of work across limb joints*

21   In human walking, the stance phase work is predominately from the ankle ($47.0 \pm$

22   6.5%), and from the hip in swing phase ($82.9 \pm 3.2\%$). This contrasts with chimpanzees

23   in which most of their positive mechanical work is from the hip in both stance ($49.1 \pm$

24   3.7%) and swing ($88.5 \pm 1.9\%$) phases (Fig. 8).

25   In stance phase, human negative work is predominately absorbed at the knee ($46.6 \pm$

26   3.0%), whereas chimpanzees absorb most of their mechanical work at the ankle ($42.4 \pm$

27   2.0%). In swing phase, the knee accounts for nearly all of the negative work in both

28   species ($H = 91.2 \pm 4.6\%$; $C = 93.0 \pm 2.1\%$).

29

30   *3.8. Dimensional vs. dimensionless walking mechanics*

14

1   For the comparison at matched dimensional speeds (i.e., absolute-speed match), the

2   average human walking speed was 1.08 ± 0.02 m s^{-1}. This corresponds to a v' of $0.36 \pm$

3   0.01 and Fr of 0.13 ± 0.02 (SOM Table S2), which are slower than the relative-speed

4   match.

5   Overall, the humans had smaller moments, work and power at matched dimensional

6   speed than at matched dimensionless speed. As such, the interspecific differences in

7   dimensional positive mechanical work and power output were consistently larger, with

8   the exception of the second double-support period positive work and power (SOM Figs.

9   S2–S8; SOM Tables S2–S5). In this case, the positive mechanical work and power output

10   were more similar between species than at the relative-speed match (SOM Fig S5). The

11   human 3-D joint moments and powers had similar profiles at 1.08 ms^{-1} and 1.66 ms^{-1}.

12   However, the magnitude of the interspecific difference in total mechanical work and

13   power were much larger (H = 83.6% vs. C = 77.8%; SOM Fig. S7) than at matched

14   dimensionless speeds, even without accounting for elastic power output. Indeed, the

15   interspecific difference in total 'muscle fiber' work and power are larger still (H =

16   106.9% vs. C = 111.9%; SOM Fig S7). This reinforces the importance of careful, speed-

17   controlled comparisons for testing the effects of musculoskeletal structure on locomotor

18   capabilities.

19

20   **4. Discussion**

21   *4.1. Ground reaction forces, stride-to-stride and intraspecific variation*

22   Our results are broadly consistent with previous descriptions of the 3-D ground force

23   components in bipedal chimpanzee walking (Kimura et al., 1977; Pontzer et al., 2009).

24   As expected, all three animals exhibited monophasic vertical force patterns, with small

25   magnitude anterior-posterior force peaks compared to a human walking step at similar

26   dimensionless speeds, especially in the second double-support period (i.e., push-off). The

27   species difference in peak vertical force magnitude (H = 1.27, C = 1.13; Fig. 2) supports

28   the inference that facultative bipeds walk with lower peak vertical force (Schmitt, 2003),

29   albeit by a small amount at matched dimensionless speeds. However, this difference is

30   not present at matched dimensional speeds (SOM Fig. S2). Overall, the ground reaction

31   forces in bipedal chimpanzees appear quite similar to the 3-D forces of 'highly-trained'

15

1   bipedal macaques (Kimura et al., 1977; Ogihara et al., 2007), as well as some other

2   facultative bipeds (Kimura, 1977). A qualitative comparison of our chimpanzee dataset to

3   similar data from 'highly-trained' bipedal macaques (Ogihara et al., 2007) suggests that

4   bipedal chimpanzees and macaques are much more similar to each other than either are to

5   humans.

6   The data herein indicate that bipedal chimpanzees exceed humans in the variation of

7   their ground reaction forces from stride to stride. Among individuals, chimpanzees are

8   more variable than humans in their anterior-posterior and medio-lateral ground forces,

9   but similar in their vertical component. These results are consistent with CMC results for

10   the pelvis and lower/hind limb 3-D kinematics reported in O'Neill et al. (2015). The

11   similarities in the vertical force CMC values suggest that the monophasic pattern is quite

12   consistent across our three subjects, as suggested by average patterns from chimpanzees

13   in earlier studies from a range of ages and body masses (Kimura et al., 1977; Pontzer et

14   al., 2009).

15

16   *4.2. Joint moments*

17   Our results are consistent with earlier 2-D data on the sagittal plane moments of

18   humans and bipedal chimpanzees throughout stance (Yamazaki et al., 1981; Sockol et al.,

19   2007). In particular, bipedal chimpanzees—like all facultative bipeds studied to date

20   (Yamazaki et al., 1981; Yamazaki, 1985)—have a substantial hip extension moment for

21   nearly the full duration of stance.

22   However, these 3-D data also provide insight into bipedal chimpanzee mechanics in

23   the non-sagittal planes, and over a full walking stride. Hip abduction-adduction moments

24   are different in magnitude and opposite in direction for human and bipedal chimpanzee

25   walking. The absence of an abductor moment in the stance phase in bipedal chimpanzee

26   walking, and throughout the single-support period in particular, provides quantitative

27   support to the longstanding view that the human 'lateral balance mechanism' is a derived

28   aspect of hominin walking (e.g., Stern and Susman, 1981; Lovejoy, 1988). The marked

29   contrast in hip abduction-adduction moments between humans and bipedal chimpanzees

30   demonstrates that the single-support period of a bipedal walking stride need not follow

31   the simple 'mechanical model' of hip loading, which assumes a large abduction moment

1   during single-support (e.g., Lovejoy et al., 1973; Ruff, 1995; see also Warrener, 2017).

2   This is an important consideration in general, but especially when extending this human-

3   based approach to the earliest hominins (e.g., Richmond and Jungers, 2008).

4   The single-support period of bipedal chimpanzees is characterized by a larger internal

5   (i.e., medial) rotation moment than in human walking. This supports the inference of

6   Stern and Susman (1981:164) that for chimpanzees, "… the problem posed during the

7   single support phase of bipedality is to prevent collapse into lateral rotation at the stance

8   side hip." Our results confirm and extend this inference, indicating that there is also a

9   substantial hip adduction moment in bipedal chimpanzee walking, which reaches a

10 similar magnitude to the internal rotation moment near the end of the single-support

11 period. Taken together, the moment data herein confirm that the distinction between the

12 3-D mechanics of the single-support period in bipedal chimpanzee and human walking is

13 a reliance on 'rotation-based' or 'rotation-adduction-based' hip mechanics in

14 chimpanzees, and 'abduction-based' hip mechanics in humans for 'maintaining lateral

15 balance'. How individual hind-limb muscle-tendon units contribute to balancing these

16 moments in bipedal chimpanzees requires additional quantitative analyses, since an

17 individual muscle-tendon unit will, in general, have non-zero moment arms about all

18 three hip joint axes that can change in magnitude and sign during movement (e.g.,

19 O'Neill et al., 2013).

20   The joint moment data also extend our earlier findings (O'Neill et al., 2015, 2018)

21 that the use of a 'heel strike' during walking in humans is distinct, not just in its

22 consistency (Elftman and Manter, 1938; Webber and Raichlen, 2016), but in both its

23 associated ankle kinematics and mechanics, despite some qualitative similarities with

24 other African apes overall (Schmitt and Larson, 1993). At the human ankle, there is a

25 consistent, net dorsiflexion moment from 'heel strike' through the first double-support

26 period, which contrasts with the net plantar flexor moment in bipedal chimpanzees. How

27 these different foot strike patterns impact ankle muscle-tendon mechanics and energetics

28 in walking is still unclear, but some limited metabolic data indicate that evolution of the

29 hominin 'heel strike' is of much greater consequence for walking than running (e.g.,

30 Cunningham et al., 2010; Gruber et al., 2013). When human-like 'heel strike' walking

31 first appeared in hominin evolution is still unclear, although a robust calcaneal tuber and

17

1   lateral plantar process has been used to infer its presence as early as *Australopithecus*

2   *afarensis* (e.g., Latimer and Lovejoy, 1989; Prang, 2015; DeSilva et al., 2019). Still, this

3   is difficult to establish even from fossil footprints such as the Laetoli site tracks (e.g.,

4   Leakey and Hay, 1979; Masao et al., 2016), since both human and bipedal chimpanzee

5   foot strikes induce relatively deep heel impressions (Hatala et al., 2016a).

6   Human and bipedal chimpanzee joint moments are broadly similar in direction and

7   magnitude throughout limb swing, except in hip internal-external rotation. This is

8   consistent with greater circumduction of the hind limb in bipedal chimpanzee walking

9   (O'Neill et al., 2015). The limb-swing rotational moments also provide some indirect

10   support to the inference of Stern and Larson (1993:425) that m. obturator externus is

11   activated "to counteract [a] medial rotatory effect" in the first half of limb swing, as there

12   is a net internal (i.e., medial) rotation moment at this time in bipedal chimpanzees.

13

14   *4.3. Mechanical work and power in stance*

15   Our results provide some support for the first hypothesis that human walking involves

16   lower work and power output in stance phase than bipedal chimpanzees. This is due, in

17   large part, to significantly less positive mechanical work and power output in the first

18   double-support and single-support periods of a human walking stride. While both humans

19   and chimpanzees absorb mechanical energy at the hip in the first double-support period,

20   there is greater net positive mechanical work at the knee (Figs. 3A, B) in bipedal

21   chimpanzee walking.

22   The greater positive mechanical work in the single-support period in chimpanzees is

23   due primarily to greater positive power at the hip, with small contributions from the knee

24   and ankle. This is consistent with previous assessments of sagittal plane hip moments,

25   which had indicated a substantial force-requirement at the hip during stance phase in

26   bipedal chimpanzees (Sockol et al., 2007; Pontzer et al., 2009). In middle single-support,

27   the lower back, pelvis and lower limbs of humans facilitate near-zero lower limb joint

28   power, followed by a short period in which mechanical energy is absorbed at the hip and

29   ankle (i.e., 'preload': Kuo et al., 2005; Zelik et al., 2015).

30

31   *4.4. Elastic work and power*

18

1   In contrast to the first double-support and single-support periods, humans markedly
2   exceed bipedal chimpanzees in total positive mechanical work and power during the
3   second double-support period due to substantial mechanical energy generation at the
4   ankle for push-off. Muscle-tendon models (e.g., Hof et al., 1983) and direct imaging of
5   muscle fiber dynamics (e.g., Fukanaga et al., 2001; Ishikawa et al., 2005; Farris and
6   Sawicki, 2012b) indicate that much of the positive power for human push-off is due to
7   the elastic recoil of the Achilles tendon, stretched during the single-support period. Based
8   on the mechanical energy absorbed at the ankle during the single-support period at this
9   speed, we estimated that $39 \pm 13\%$ of the positive power for ankle push-off is from
10   elastic storage, on average (Fig 5). The upper error margin of our indirect, inverse
11   dynamics-based approximation overlaps direct imaging of muscle fiber behavior in
12   humans walking between 1.25 and 1.75 ms^{-1}, which indicates a significant contribution
13   from elastic power (i.e., 50 to 55%), at least for m. gastrocnemius (Farris and Sawicki,
14   2012b). It has been reported that the typical procedures used in direct imaging studies can
15   overestimate the elastic energy returned from tendons (Zelik and Franz, 2017), which
16   may account for some of the difference in mean values. Of course, both these indirect and
17   direct estimates are subject to the limitations of the inverse-dynamics approach and
18   would benefit from continued refinement using detailed musculoskeletal models that
19   account for individual muscle-tendon unit behavior (e.g., Hornet and Zelik, 2016).

20   The contribution of elastic positive hip work to the second double-support period and
21   limb swing is less well understood but has been estimated to be 10–58% across a range of
22   walking speeds (Yoon and Mansour, 1982; Varhas et al., 1990; Whittington et al. 2008).
23   Herein, we estimated that the human hip stored and released $25.5 \pm 10.7\%$ of the positive
24   work to the second double-support period and limb swing, which is in the middle of this
25   published range. Hip joint capsular ligaments and associated tissues have long been
26   identified as a source of hip elastic work (e.g., Neptune et al., 2008; Whittingon et al.,
27   2008), since the anterior tissues (e.g., iliofemoral ligament) will be strained during hip
28   extension. The iliotibial tract, which has a hip flexion moment arm, appears to contribute
29   as well (Eng et al., 2015). Direct imaging of hip flexor muscle fiber behavior (e.g., rectus
30   femoris) would help elucidate the role of muscle and tendon to positive power output in
31   the second double-support and limb swing periods of a human walking stride.

1   Over a full stride, our estimated total elastic work contributions (i.e., ankle and hip: 2 $24.2 \pm 3.1\%$ at 1.66 ms^{-1}; $31.1 \pm 7.2\%$ at 1.08 ms^{-1}) is similar to the series elastic element 3   contributions to the total lower limb work from individual muscle tendon dynamics (e.g., 4   29.4% tendon elastic work to muscle fiber work at 1.2 ms^{-1}: Sasaki et al. 2009). This 5   suggests that our estimates are reasonable initial approximations. It is well known that net 6   joint-level measures do not equate to total muscle-tendon unit work and power, owing to 7   bi-articular muscle recruitment and muscle co-contraction (Sasaki et al. 2009), which 8   may differ between human and bipedal chimpanzee walking.

9   The hind limb joint mechanics and muscle-tendon structure of bipedal chimpanzees 10   suggest a limited capacity for elastic work and power output in a walking stride. First, the 11   joint mechanics data herein demonstrate that, unlike human walking, the second half of 12   the single-support period of chimpanzee bipedal walking involves no net negative hip or 13   ankle work (see Fig. 4 and SOM Fig. S4) for elastic energy storage and is instead a 14   continuous period of positive work. The absence of this negative work suggests that there 15   is no significant elastic contribution from the hip and ankle to 'push-off' in bipedal 16   chimpanzees. This is also implied by the hip flexion-extension range of motion, which is 17   about half that of humans (O'Neill et al., 2015: C: 27°; H: 48°), indicating less capacity 18   for hip tissue strain and elastic energy storage overall. Indeed, the passive tissue strain 19   and elastic work of the iliotibial tract of bipedal chimpanzees has been estimated to be 20   only a small fraction of human values (Eng et al., 2015), due in large part to this 21   kinematic difference. Second, chimpanzee pelvis and hind limb muscles are also 22   characterized by relatively longer muscle fibers than human lower limb muscles, and the 23   near absence of a free Achilles tendon (e.g., Thorpe et al., 1999; O'Neill et al., 2013, 24   2017). Chimpanzee pelvis and hind limb relative muscle fiber lengths (i.e., ratio of 25   muscle fiber length to total muscle-tendon unit length) are about 15% longer than humans 26   overall (C = 0.59 ± 0.21, H = 0.44 ± 0.25), and about twice as long for the leg/shank 27   muscles in particular (C = 0.33 ± 0.14, H = 0.15 ± 0.04; Arnold et al., 2010; O'Neill et 28   al., 2013; see also Thorpe et al., 1999). This architectural design requires the muscle 29   fibers to more closely track the muscle-tendon length changes due to the joint motions, 30   implying a limited capacity for tendon strain and thus storage and release of elastic 31   energy. Still, short, stiff tendons, long, thin internal tendons and sarcomeric proteins may

1 permit some degree of elastic work and power output (e.g., Alexander, 1988; Roberts,

2 2016). Decomposition of joint-level 3-D mechanics among individual muscles and series

3 elastic elements via optimization can provide a more detailed accounting of the muscle-

4 tendon mechanical work and power (e.g., Anderson and Pandy, 1993, 2001), and more

5 precise estimates of the elastic contribution to human and bipedal chimpanzee walking.

6

7 *4.5. Mechanical work and power in limb swing*

8   Our results also provide some limited support for our second hypothesis that human

9 limb structure reduces limb swing positive work and power. The greater positive work

10 and, to a lesser extent, power in bipedal chimpanzee limb swing is consistent with the

11 hypothesized differences in limb structure. However, it is difficult to isolate the

12 contribution of the limb-mass distribution per se. This is because bipedal chimpanzees

13 engage in more hip rotation about abducted, flexed hind limbs throughout limb swing

14 (O'Neill et al. 2015), for reasons likely independent of limb-mass distribution. Increasing

15 limb flexion (Wu and Kuo, 2016) and circumduction (Shorter et al., 2017) in limb swing

16 increases limb joint work and positive power over a stride in human perturbation studies,

17 regardless of limb-mass distribution.

18   Elastic work and power from the hip likely contribute to both the second double-

19 support period and the first half of limb swing in human walking. Given the sinusoidal

20 shape of the positive power burst at the hip that peaks at the stance-swing transition (Fig.

21 5A), we can estimate that about half of the hip elastic work and power is output for limb

22 swing, which would further increase the human-chimpanzee limb swing differential. In

23 contrast, in the second double-support period of bipedal chimpanzee walking, the hip is

24 insufficiently extended (i.e., 25° of hip flexion, on average; O'Neill et al., 2015) to strain

25 the associated elastic tissues and permit a positive elastic power contribution to the first

26 half of limb swing. This suggests a distinct contribution of human hip mechanics during

27 the single and second double-support periods to reducing limb swing work and power,

28 independent of limb-mass distribution.

29

30 *4.6. Total mechanical work and power*

21

1   On average, human walking involves 23.3% and 12.0% less positive mechanical

2   work and power than bipedal chimpanzees, respectively. These differentials are enhanced

3   by human capacities for elastic work and power output over a stride, which are assumed

4   to be zero in bipedal chimpanzees herein. Together, these results support our third

5   hypothesis, as the total 'muscle fiber' work and power output of the human lower limb is

6   46.9% and 35.8% lower than the hind limbs of bipedal chimpanzees walking at matched

7   dimensionless speeds. This is consistent with the broad-sense expectation that our mobile

8   lower back, pelvis and long lower limbs with short feet of humans reduce the total

9   mechanical work and power output of our walking stride when compared to bipedal

10   chimpanzees; however, decomposing the individual contributions of specific traits to

11   these joint-level differences is complex, and requires additional investigation.

12   Our total mechanical power differential accounts for some, but not all, of the

13   differential in the metabolic cost of walking between humans and bipedal chimpanzees

14   (i.e., 50 to 75%: Sockol et al., 2007; Pontzer et al., 2014). Of course, joint-level metrics

15   do not account for differences in muscle co-contraction, muscle contractile behavior (i.e.,

16   force-length-velocity dynamics), muscle architecture and myosin heavy chain content

17   between species (e.g., O'Neill et al., 2013, 2017), all of which can further increase the

18   human-chimpanzee differential. For example, the relatively small, mobile limb joints of

19   chimpanzees (e.g., Jungers, 1988) may require higher levels of muscle co-contraction for

20   joint stabilization over a bipedal walking stride. In our view, model-based approaches

21   that permit optimization of individual muscle mechanics and metabolic costs can improve

22   upon previous joint-level 'force-based approximations' of muscle energy use (e.g.,

23   Roberts et al., 1998; Sockol et al., 2007; Pontzer et al., 2009), since they parameterize

24   individual-muscle excitation patterns as well as the metabolic costs of activation, cross-

25   bridge cycling, shortening-lengthening and associated contractile element dynamics (e.g.,

26   Umberger and Rubenson, 2011).

27

28   *4.7. Distribution of work and power across the limb joints*

29   In humans, positive mechanical work and power output has been shifted to the distal

30   joints, with 47% of the work performed at the ankle throughout stance phase. Notably,

31   this facilitates the use of shorter muscle fibers (Thorpe et al., 1999; Arnold et al., 2010;

1   O'Neill et al., 2013, 2017) and a greater reliance on elastic energy storage and release at
2   the ankle. Both humans and chimpanzees have relative muscle fiber lengths (i.e., ratio of
3   muscle fiber length to total muscle-tendon unit length) that are more than twice as long
4   for pelvis and thigh muscles (H = 0.55 ± 0.15, C = 0.67 ± 0.20) as for leg muscles (H =
5   0.15 ± 0.04, C = 0.33 ± 0.14; Arnold et al., 2010; O'Neill et al., 2013; see also Thorpe et
6   al., 1999). Our enlarged m. soleus and long Achilles tendon (e.g., O'Neill et al., 2013), in
7   particular, are likely derived traits within the hominin lineage that enhance our positive
8   push-off mechanics as well as elastic energy storage and release. Bipedal chimpanzees
9   have a more proximal distribution of limb work, with 49% performed at the hip during
10 stance. A reliance on proximal joints for positive work and power necessitates the
11 activation of longer, parallel-fibered muscles (e.g., Thorpe et al., 1999; O'Neill et al.,
12 2013), whose shortening-lengthening behavior is expected to more faithfully track 3-D
13 joint motion, with less capacity for decoupling of muscle fiber and tendon strain. In limb
14 swing, both humans and bipedal chimpanzees primarily use the hip. To the extent that the
15 longer, heavier feet of chimpanzees affect their limb swing mechanics, this may account
16 for some of the relatively larger contribution of hip (H = 83%, C = 89%) work (Fig. 8) in
17 bipedal chimpanzees than humans.

18   Over a steady, level walking stride, no net mechanical work is performed on the
19 environment, and the total whole-body positive and negative work must sum to zero. In
20 humans, muscle-tendon units of the lower limb provide most of the positive work through
21 rotations of the joints; however, soft tissues such as the heel pad, intervertebral discs or
22 articular cartilages likely compress and perform significant negative work on the body
23 without rotating the lower limb joints (Zelik and Kuo, 2013; Zelik et al., 2015). Our
24 results indicate that humans exhibit an imbalance of limb joint work, with average
25 negative-to-positive ratios of 67 ± 9% per step (i.e., excluding limb swing). This is nearly
26 identical to ratio of 68% per step in level walking in DeVita et al. (2007). At matched
27 dimensionless speeds, bipedal chimpanzee negative-to-positive work is more balanced,
28 with a ratio of 88 ± 8% per step. This is due to greater negative work—and more active
29 muscle-tendon unit lengthening—in bipedal chimpanzee than human walking. Although
30 the metabolic cost of performing negative muscle fiber work is low (Woledge et al.,
31 1985), energy dissipation through soft tissue deformations has no cost at all. As an

1 example, a human-like heel strike permits mechanical energy dissipation *via* the heel pad

2 (e.g., Baines et al., 2018; Honert and Zelik, 2019), rather than muscle-tendon

3 lengthening. The shift from facultative to habitual bipedal walking in hominin evolution

4 may have increased our reliance on soft (non-muscular) tissues for mechanical energy

5 dissipation, which may have some metabolic and fatigue-resistance benefits in walking

6 overall.

7

8 *4.8. Limitations of this study*

9 Studies of the development of human walking mechanics indicate that children over

10 the age of 5 years have adult-like gait mechanics and metabolic costs, once differences in

11 size are accounted for (Sutherland, 1997; Stansfield et al., 2003; Weyand et al., 2010).

12 Chimpanzees grow into adults at a faster rate than humans (Zihlman et al., 2004), but are

13 still sub-adult between the ages of 5 and 6 years old. Ontogenetic studies of chimpanzee

14 bipedal walking ground reaction forces indicated that by the age of 5, chimpanzees

15 exhibit adult-like mechanics, independent of speed (Kimura, 1996). Sagittal plane hip,

16 knee and ankle joint moments of bipedal chimpanzees that range in age from 6 to 33

17 years old were all quite similar to each other (Pontzer et al., 2014). A qualitative

18 comparison of our ground reaction forces and sagittal plane moments during stance phase

19 to these data indicates that our results are similar to chimpanzees across a broad age and

20 size range and, given the commonalities in the between-subject CMCs for both the force

21 and kinematic results (Table 2; O'Neill et al., 2015) as well, should therefore be

22 representative of bipedal chimpanzee walking in general.

23 Our analyses did not quantify intrinsic foot motion. Bipedal chimpanzees walk with

24 less 3-D midfoot (Holowka et al. 2017) and forefoot (Fernandez et al., 2016) motion than

25 humans. These new data indicating greater intrinsic foot motion in humans than bipedal

26 chimpanzees were unexpected given long-standing dichotomies of human feet as 'stiff'

27 and chimpanzees as 'mobile' in bipedal walking (e.g., Elftman and Manter, 1935;

28 Susman, 1983). However, the 'stiff' and 'mobile' dichotomy may be more reflective of

29 passive ranges of motion as well as an overemphasis on the 'midtarsal break' in the

30 single-support period of bipedal chimpanzee walking. Indeed, most of human 3-D

31 midfoot and forefoot motion actually occurs in the second double-support period, not in

the single-support period (e.g., Lundgren et al. 2003; Holowka et al. 2015). Our inverse kinematics weighted markers located on the calcaneus more heavily than other foot markers for calculating ankle joint kinematics, which keeps intrinsic foot deformation from contaminating ankle joint angular velocities, and therefore ankle joint power. This approach helps prevent overestimation of 'push-off' power, which is important for proper calculation of plantar flexor muscle function (e.g., Zelik and Hornet, 2018). Still, we did not take into account the possible intrinsic foot power generation in late stance. Greater human intrinsic foot motion may have some adaptive value in contributing positive power to push-off (e.g., Takahashi et al., 2017; Farris et al., 2019; but also see Zelik et al., 2015). The limited midfoot and forefoot motion, together with small peak forces in the second double-support period of bipedal chimpanzee walking (see Fig. 2) suggest little foot positive power in push-off, by comparison. Thus, the inclusion of intrinsic foot mechanics in comparisons of human and bipedal chimpanzee walking may affect the total limb power output and is an important area of future study for understanding hominin foot evolution.

4.9. Implications for fossil hominin bipedal biomechanics

The single-support period of a walking stride has particular relevance for hominin evolution since a number of skeletal traits have been tied to 'maintaining lateral balance' in hominins, such as ilia orientation (e.g., Stern and Susman, 1981; Lovejoy, 1988). Humans are well known to use an 'abductor-based hip mechanism' in the single-support period, an assumption that has been extended to a wide range of fossil hominins (e.g., Lovejoy et al., 1973; Ruff, 1995), including the earliest hominins (e.g., Richmond and Jungers, 2008). Our results demonstrate that bipedal chimpanzees use an alternate mechanism, in which there are large internal rotation and adduction moments in the single-support period. This 'rotation-based' or 'rotation-adduction-based' mechanism for 'maintaining lateral balance' confirms and extends the inferences of Stern and Susman (1981), who proposed these single-support period mechanics for bipedal chimpanzees and other apes (i.e., gibbons, orangutans). This represents an alternative means of maintaining whole-body stability during bipedal walking; one that likely preceded the 'abductor-based' mechanism in the hominin lineage. Indeed, the likelihood that the

1   kinematics and mechanics of bipedal walking at the origins of hominin lineage were quite

2   distinct from humans and much more similar to bipedal walking in facultative bipeds (cf.

3   O'Neill et al., 2018) is an important consideration when searching for skeletal adaptations

4   for 'terrestrial bipedal travel' in the earliest putative hominins (e.g., Macchiarelli et al.,

5   2020). More experimental and modeling-simulation studies are needed to evaluate how

6   musculoskeletal trait evolution in the pelvis and hind/lower limbs, including shifts in ilia

7   length and orientation (e.g., Stern and Susman, 1981; Lovejoy, 1988) facilitate the use of

8   an 'adduction-based mechanism' for 'maintaining lateral balance'.

9   An important difference in musculoskeletal structure between humans and

10   chimpanzees is that chimpanzees possess a longer ischium than humans (e.g., Stern and

11   Susman, 1983; Lovejoy, 1988). A long ischium is evident in *Ar. ramidus* at 4.4. million

12   years ago (Lovejoy et al. 2009), as well as all Miocene apes with associated pelvis

13   remains (Hammond et al., 2013, 2020; Morgan et al., 2015; Ward, 1993; Ward et al.,

14   2019). Komza et al. (2018:4136) has recently proposed that shortening the ischium in

15   hominin evolution facilitated 'hamstrings-powered hip extension'. However, our results

16   demonstrate that the second-double support period in a human walking stride is

17   associated with a net flexion moment at the hip, not a net extension moment (cf. Fig. 3

18   and SOM Fig. S3). As such, the net mechanical energy generated during the second-

19   double support period at the human hip is not due to 'hamstrings power', but instead to

20   substantial hip flexor muscle (e.g., m. iliopsoas; Capellini et al., 2006) and elastic power.

21   Indeed, in both human and bipedal chimpanzee walking, the hamstring muscles (i.e., mm.

22   semimembranosus, semitendinosus and biceps femoris, long head) are quiescent in late

23   stance (e.g., Winter and Yak, 1987; Capellini et al., 2006; Schmitz et al., 2009; Larson

24   and Stern, unpublished data). Instead, our results indicate that a shorter ischium in

25   humans is associated with greater hip extension than bipedal chimpanzees in the second

26   half of the single-support and double-support periods, which permits a passive elastic

27   contribution at the hip, thereby contributing positive power through push-off into limb

28   swing.

29   Our results demonstrate significant differences between humans and bipedal

30   chimpanzees over a full walking stride but place new emphasis on the second half of the

31   single support period (i.e., for elastic tissues strain) and the second-double support period

26

1   (i.e., for push-off) for the evolution of hominin walking. An abducted hallux in *Ar.*

2   *ramidus* (Lovejoy et al., 2009b; Simpson et al., 2019; see also Haile-Selassie et al., 2012)

3   suggests that the earliest hominins still utilized a relatively weak push-off in the double-

4   support period at 4.4 Mya, quite distinct from human walking. Lovejoy et al. (2009b) has

5   proposed that, in the absence of an adducted hallux, the center of pressure was directed

6   along the full length of the foot and through the more lateral phalanges in *Ar. ramidus*. In

7   bipedal chimpanzees, the center of pressure remains proximal to the phalanges over a

8   walking step, including during the second double-support period (see Fig 1; see also

9   Vereecke et al. 2003). Skeletal correlates of an enhanced capacity for

10 metatarsophalangeal flexion in digits 2–4 in *Ar. ramidus* compared to African apes

11 (Lovejoy et al., 2009b; Fernández et al., 2018; Simpson et al., 2019), raise the possibility

12 of a more distal progression of the center of pressure than in bipedal chimpanzees;

13 however, the lateral digits still lack the structural integrity of a large hallux for applying a

14 substantial push-off impulse via the ankle plantar flexors (and, to a lesser extent, the

15 intrinsic foot tissues: Takahashi et al., 2017). Nevertheless, this may represent some

16 improvement over the limited capabilities of bipedal chimpanzees or a *Pan-Homo* last

17 common ancestor with an African ape-like foot (e.g., Pilbeam and Lieberman, 2017;

18 Prang, 2019). A more adducted hallux is evident in *Au. afarensis* (e.g., Susman et al.,

19 1984; DeSilva et al., 2019) as well as the associated Lateoli site G and site S footprints

20 (Leakey and Hay, 1979; Masao et al., 2016), although the substantial positive power at

21 the ankle via a human-like push-off may not appear until *Homo* (e.g., Fernández et al.,

22 2016, 2018). Indeed, the differences between the ca. 3.7 Mya Laetoli footprints and the

23 1.5 Mya Ileret footprints may reflect this (Bennett et al., 2009; Hatala et al., 2016b; but

24 see Raichlen and Gordon, 2017). More experimental-modeling studies of the effects of

25 foot musculoskeletal structure on push-off mechanics in walking are needed to clarify

26 these issues.

27

28 **5. Conclusions**

29   The analyses presented herein provide the first description of the 3-D hip, knee and

30 ankle moments, work, and power of bipedal chimpanzees, and direct comparisons to

31 humans walking at matched dimensionless and dimensional speeds over a full walking

1   stride. They provide partial or full support for our three main hypotheses relating
2   musculoskeletal structure to mechanics across a full walking stride.

3   Still, it is difficult to decompose the individual contributions of musculoskeletal traits
4   such as a mobile lower back, a short pelvis, and long lower limbs and short feet via joint-
5   level analyses alone. Additional contributions from differences in upper body size and
6   shape or neural control may also be relevant. Yet, this is a necessary step for linking the
7   hominin fossil record to shifts in hominin walking capabilities. As such, future research
8   should use the results herein to investigate the effects of isolated traits, both skeletal (e.g.,
9   ilia orientation, hallux adduction) and soft tissue (e.g., m. soleus, Achilles tendon), on the
10   mechanics of human walking (e.g., single support, 'push-off', etc.) and across lower limb
11   joints over a stride. While studies of isolated traits in hominin evolution have historically
12   been approached using either comparative morphology or, to a much lesser extent,
13   experimentation in living taxa (e.g., Ross et al., 2002), there is an increasingly viable and
14   important role for computer simulation and optimization methods to establish direct
15   cause-and-effect relationships based on high-fidelity models of the neuromusculoskeletal
16   systems (e.g., Falisse et al., 2019). This approach may be especially useful for testing the
17   adaptive nature of trait combinations not present in living species or along a single
18   lineage, such as hominins. High-quality, controlled experimental data, such as the force,
19   moment, work, and power measurements of humans and bipedal chimpanzees herein,
20   provide the experimental basis for these studies.

1   **References**

2   Alexander, R.M., 1988 Elastic Mechanisms in Animal Movement. Cambridge University
3   Press. Cambridge, UK.
4

5   Alexander, R.M., 1989 Optimization and gaits in the locomotion of vertebrates. Physiol.
6   Rev. 69, 1199-1227.
7

8   Anderson, F.C., Pandy, M.G., 1993. Storage and utilization of elastic strain energy during
9   jumping. J. Biomech. 26, 1413-1427.
10

11 Anderson, F.C., Pandy, M.G., 2001. Static and dynamic optimization solutions for gait
12   are practically equivalent. J. Biomech. 34, 153-161.
13

14 Arnold, E.M., Delp, S.L. 2011., Fibre operating lengths of human lower limb muscles
15   during walking. Philos. Trans. R. Soc. Lond. B. Biol. Sci. 366, 1530-1539.
16

17 Arnold, E.M., Ward, S.R., Lieber, R.L., Delp, S.L., 2010. A model of the lower limb for
18   analysis of human movement. Ann. Biomed. Eng. 38, 269-279.
19

20 Arnold, E.M., Hamner, S.R., Seth, A., Millard, M., Delp, S.L., 2013. How muscle fiber
21   lengths and velocities affect muscle force generation as humans walk and run at
22   different speeds. J. Exp. Biol. 216, 2150-2160.
23

24 Baines, P.M., Schwab, A.L., van Soest, A.J., 2018. Experimental estimation of energy
25   absorption during heel strike in human barefoot walking. PLoS One 13,
26   e0197428.
27

28 Bennett, M., Harris, J., Richmond, B., Brain, D., Mbua, E., Kiura, P., Olago, D.,
29   Kibunija, M., Omuombo, C., Behrensmeyer, A.K., Huddart, D., Gonzalez, S.,
30   2009. Early hominin foot morphology based on 1.5-million-year-old footprints
31   from Ileret, Kenya. Science 323, 1197–1201.
32

33 Browning, R.C., Modica, J.R., Kram, R., Goswami, A., 2007. The effects of adding mass
34   to the legs on the energetics and biomechanics of walking. Med Sci. Sports Exerc.
35   39, 515-525.
36

37 Cappellini, G., Ivanenko, Y.P., Poppele, R.E., Lacquaniti, F., 2006. Motor patterns in
38   human walking and running. J. Neurophysiol. 95, 3426-3437.
39

40 Cunningham, C.B., Schilling, N., Anders, C., Carrier, D.R., 2010. The influence of foot
41   posture on the cost of transport in humans. J. Exp. Biol. 213, 790-797.
42

43 Delp, S.L., Loan, J.P., Hoy, M.G., Zajac, F.E., Topp, E.L., Rosen, J.M., 1990 An
44   interactive graphics-based model of the lower extremity to study orthopaedic
45   surgical procedures. IEEE Trans. Biomed. Eng. 37, 757-767.
46

1   Delp, S.L., Anderson, F.C., Arnold, A.S., Loan, P., Habib, A., John, C.T., Guendelman,
2   E., Thelen, D.G., 2007 OpenSIM: Open-source software to create and analyze
3   dynamic simulations of movement. IEEE Trans. Biomed. Eng. 54, 1940-1950.

5   DeSilva, J., McNutt, E., Benoit, J., Zipfel, B., 2019. One small step: A review of Plio-
6   Pleistocene hominin foot evolution Yearbk. Phys. Anthropol. 168, 63-140.

8   DeVita, P., Helseth, J., Hortobagyi, T., 2007. Muscles do more positive than negative
9   work in human locomotion. J. Exp. Biol. 210, 3361-3373.

11   Elftman, H., Manter, J., 1935 Chimpanzee and human feet in bipedal walking. Am. J.
12   Phys. Anthropol. 1, 69-79.

14   Eng, C.M., Arnold, A.S., Biewener, A.A., Lieberman, D.E., 2015. The human iliotibial
15   band is specialized for elastic energy storage compared with the chimp fascia lata.
16   J. Exp. Biol. 218, 2382-2393.

18   Eng, J.J., Winter, D.A., 1995. Kinetic analysis of the lower limbs during walking: What
19   information can be gained from a three-dimensional model? J. Biomech. 28, 753-
20   758.

22   Falisse, A., Serrancoli, G., Dembia, C.L., Gillis, J., Jonkers, I., De. Groote, F., 2019.
23   Rapid predictive simulations with complex musculoskeletal models suggest that
24   diverse healthy and pathological human gaits can emerge from similar control
25   strategies. J. R. Soc. Interface 16, 20190402.

27   Farris, D.J., Sawicki, G.S., 2012a. The mechanics and energetics of human walking and
28   running: A joint level perspective. J. R. Soc. Interface 9, 110-118.

30   Farris, D.J., Sawicki, G.S., 2012b. Human medial gastrocnemius force-velocity behavior
31   shifts with locomotion speed and gait. Proc. Natl. Acad. Sci. USA 109, 977-982.

33   Farris, D.J., Kelly, L.A., Crewsell, M.A., Litchwark, G., 2019. The functional importance
34   of human foot muscles for bipedal locomotion. Proc. Natl. Acad. Sci. USA 116,
35   1645-1650.

37   Field, A., 2013. Discovering Statistics Using IBM SPSS Statistics, 4th edition. Sage,
38   London.

40   Fernández, P.J., Holowka, N.B., Demes, B., Jungers, W.L., 2016. Form and function of
41   the human and chimpanzee forefoot: Implications for early hominin bipedalism.
42   Sci. Rep. 6, 30532.

44   Fernández, P.J., Mongle, C.S., Leakey, L., Proctor, D.J., Orr, C.M., Patel, B.A.,
45   Almécija, S., Tocheri, M.W., Jungers, W.L., 2018. Evolution and function of the
46   hominin forefoot. Proc. Natl. Acad. Sci. USA 115, 8746-8751.

Fukunaga, T., Kubo, K., Kawakami, Y., Fukashiro, S., Kanehisa, H., Maganaris, C.N., 2001. In vivo behavior of human muscle tendon during walking. Proc. R. Soc. Lond. B Biol. Sci. 268, 229-233.

Gray, J., 1968. Animal Locomotion. W.W. Norton & Co, Inc., New York.

Gruber, A.H., Umberger, B.R., Braun, B., Hamill, J., 2013. Economy and rate of carbohydrate oxidation during running with rearfoot and forefoot strike patterns. J Appl. Physiol. 115, 194-201.

Hammond, A.S., Alba, D.M., Almécija, S., Moyà-Solà, S., 2013. Middle Miocene *Pierolapithecus* provides a first glimpse into early hominid pelvic morphology. J. Hum. Evol. 64, 658–666.

Hammond, A.S., Rook, L., Anaya, A.D., Cioppi, E., Costeur, L., Moyà-Solà, S., Almécija, S., 2020. Insights into the lower torso in late Miocene hominoid *Oreopithecus bambolii*. Proc. Natl. Acad. Sci. USA 117, 278-284.

Hatala, K.G., Demes, B., Richmond, B.G., 2016a. Laetoli footprints reveal bipedal gait biomechanics different from those of modern humans and chimpanzees. Proc. R. Soc. Lond. B Biol. Sci. 283, 20160235.

Hatala, K.G., Roach, N.T., Ostrofsky, K.R., Wunderlich, R.E., Dingwall, H.L., Villmoare, B.A., Green, D.J., Harris, J.W.K., Braun, D.R., Richomond, B.G., 2016b. Footprints reveal direct evidence of group behavior and locomotion in *Homo erectus*. Sci. Rep. 6, 28766.

Haile-Selassie, Y., Saylor, B.Z., Deino, A., Levin, N.E., Alene, M., Latimer, B., 2012. A new hominin foot from Ethiopia shows multiple Pliocene bipedal adaptations. *Nature* 483, 565-569.

Hildebrand M. 1985. Walking and running. In: Hildebrand, M., Bramble, D.M., Liem, K.F., Wake, D.B. (Eds.), Functional Vertebrate Morphology. Harvard University Press, Boston, pp. 38-57

Hof, A.L., Geelen, B.A., van den Berg, J.W., 1983. Calf muscle moment, work and efficiency in level walking: Role of series elasticity. J. Biomech. 16, 523-537.

Holowka, N.B., O'Neill, M.C., Thompson, N.E., Demes, B., 2017. Chimpanzee and human midfoot motion during bipedal walking and the evolution of the longitudinal arch of the foot. J. Hum. Evol. 104, 23-31.

Honert, E.C., Zelik, K.E., 2016. Inferring muscle-tendon unit power from ankle joint power during the push-off phase of human walking: Insights from a multiarticular EMG-driven model. PLoS One 11, e0163169.

Honert, E.C., Zelik, K.E., 2019. Foot and shoe responsible for the majority of soft tissue work in early stance of walking. Hum. Mov. Sci. 64, 191-202.

Ishikawa, M., Komi, P.V., Grey, M.J., Lepola, V., Bruggemann, G-P., 2005. Muscle-tendon interaction and elastic energy usage in human walking. J. Appl. Physiol. 99, 603-608.

Isler, K., Payne, R.C., Gunther, M.M., Thorpe, S.K.S., Savage, R., Crompton, R.H., 2006. Inertial properties of hominoid limb segments. J. Anat. 209, 201-218.

Jungers, W.L., 1988. Relative joint size and hominoid locomotor adaptations with implications of the evolution of hominid bipedalism. J. Hum. Evol. 17, 247-265.

Jungers, W.L., Stern, J.T., Jr., 1988. Body proportions, skeletal allometry and locomotion in the Hadar hominids: A reply to Wolpoff. J. Hum. Evol. 12, 673-684.

Kadaba, M.P., Ramakrishnan, H.K., Wooten, M.E., Gainey, J., Gorton, G., Cochran, G.V.B., 1989. Repeatability of kinematic, kinetic, and electromyographic data in normal adult gait. J. Ortho. Res. 7, 849-860.

Kimura, T., 1996. Centre of gravity of the body during the ontogeny of chimpanzee bipedal walking. Folia Primatol. 66, 126-136.

Kimura, T., Okada, M., Ishida, H., 1977. Dynamics of primate bipedal walking as viewed from the force of foot. Primates 18, 137-147.

Komza, E.E., Webb, N.M., Harcourt-Smith, W.E.H., Raichlen, D.A., D'Août, K., Brown, M.H., Finestone, E.M., Ross, S.R., Aerts, P., Pontzer, H., 2018. Hip extensor mechanics and the evolution of walking and climbing capabilities in humans, apes and fossil hominins. Proc. Natl. Acad. Sci. USA 115, 4134-4139.

Kram, R., Domingo, A., Ferris, D.P., 1997 Effect of reduced gravity on the preferred walk-run transition speed. J. Exp. Biol. 200, 821-826.

Kuo, A.D., Donelan, J.M., Ruina, A., 2005. Energetic consequences of walking like an inverted pendulum: Step-to-step transitions. Exerc. Sport Sci. Rev. 33, 88-97.

Latimer, B., Lovejoy, C.O., 1989. The calcaneus of *Australopithecus afarensis* and its implications for the evolution of bipedality. Am. J. Phys. Anthropol. 78, 369-386.

Leakey, M.D., Hay, R.L., 1979. Pliocene footprints in the Laetoli beds and Laetoli, northern Tanzania. Nature 278, 317-323.

Lovejoy, C.O., 1988 Evolution of human walking. Sci. Am. 259, 118-125.

1   Lovejoy, C.O., Suwa, G., Spurlock, L., Asfaw, B., White, T.D., 2009a. The pelvis and
2   femur of *Ardipithecus ramidus*: The emergence of upright walking. Science 326,
3   71e1-71e6.
4
5   Lovejoy, C.O., Latimer, B., Suwa, G., Asfaw, B., White, T.D., 2009b Combining
6   prehension and propulsion: The foot of *Ardipithecus ramidus*. Science 326, 72e1-
7   72e8.
8
9   Lovejoy, C.O., Latimer, B.M., Spurlock, L., Haile-Selassie, Y., 2016. The pelvic girdle
10   and limb bones of KSD-VP-1/1. In: Haile-Selassie, Y., Su, D.F. (Eds.), The
11   Postcranial Anatomy of *Australopithecus afarensis*: New Insights from KSD-VP-
12   1/1. Springer, New York, pp. 155-178.
13
14 Lu, T.W., O'Connor, J.J., 1999. Bone position estimation from skin marker coordinates
15   using global optimization with joint constraints. J. Biomech. 32, 129-134.
16
17 Lundgren, P., Nester, C., Liu, A., Arndt, A., Jones, R., Stacoff, A., Wolf, P., Lundberg,
18   A., 2008. Invasive in vivo measurement of rear-, mid- and forefoot motion during
19   walking. Gait Posture 28, 93-100.
20
21 Macchiarelli, R., Bergeret-Medina, A., Marchi, D., Wood, B., 2020. Nature and
22   relationships of *Sahelanthropus tchadensis*. J. Hum. Evol. 149, 102898.
23
24 Masao, F.T., Ichumbaki, E.B., Cherin, M., Barili, A., Boschian, G., Iurino, D.A.,
25   Menconero, S., Moggi-Cecchi, J., Manzi, G., 2016. New footprints from the
26   Laetoli (Tanzania) provide evidence for marked body size variation in early
27   hominins. eLife 5, e19568.
28
29 Morgan, M.E., Lewton, K.L., Kelley, J., Otárola-Castillo, E., Barry, J.C., Flynn, L.J.,
30   Pilbeam, D., 2015. A partial hominoid innominate from the Miocene of Pakistan:
31   Description and preliminary analyses. Proc. Natl. Acad. Sci. USA 112, 82-87.
32
33 Neptune, R.R., Sasaki, K., Kautz, S.A., 2008. The effect of walking speed on muscle
34   function and mechanical energetics. Gait Posture 28, 135-143.
35
36 Ogihara, N., Hirasaki, E., Kumakura, H., Nakatuskasa, M., 2007. Ground-reaction-force
37   profiles of bipedal walking in bipedally trained Japanese monkeys. J. Hum. Evol.
38   53, 302-308.
39
40 Ogihara, N., Makishima, H., Nakatsukasa, M., 2010. Three-dimensional musculoskeletal
41   kinematics during bipedal locomotion in the Japanese macaque, reconstructed
42   based on an anatomical model-matching method. J. Hum. Evol. 58, 252-261.
43
44 Okada, M., 1985. Primate bipedal walking: Comparative kinematics. In: Kondo, S. (Ed.),
45   Primate Morphophysiology, Locomotor Analyses, and Human Bipedalism.
46   University of Tokyo Press, Tokyo, pp. 47-58.

33

O'Neill, M.C., Lee, L-F., Larson, S.G., Demes, B., Stern, J.T., Jr., Umberger, B.R., 2013. A three-dimensional musculoskeletal model of the chimpanzee (*Pan troglodytes*) pelvis and hind limb. J. Exp. Biol. 216, 3709-3723.

O'Neill, M.C., Lee, L-F., Demes, B., Thompson, N.E., Larson, S.G., Stern, J.T., Jr., Umberger, B.R., 2015. Three-dimensional kinematics of the pelvis and hind limbs in chimpanzee (*Pan troglodytes*) and human bipedal walking. J. Hum. Evol. 86, 32-42.

O'Neill, M.C., Umberger, B.R., Holowka, N.B., Larson, S.G., Reiser, P.J., 2017. Chimpanzee super strength and human skeletal muscle evolution. Proc. Nat. Acad. Sci. USA 114, 7343-7348.

O'Neill, M.C., Demes, B., Thompson, N.E., Umberger, B.R., 2018. Three-dimensional kinematics and the origin of the hominin walking stride. J. R. Soc. Interface 15, 20180205.

Pilbeam, D.R., Lieberman, D.E., 2017. Reconstructing the last common ancestor of chimpanzees and humans. In: Muller, M.N., Wrangham, R.W., Pilbeam, D.R. (Eds.), Chimpanzees and Human Evolution. Harvard University Press, Cambridge, pp 22-141.

Pontzer, H., Raichlen, D.A., Sockol, M.D., 2009. The metabolic cost of walking in humans, chimpanzees and early hominins. J Hum. Evol. 56, 43-54.

Pontzer, H., Raichlen, D.A., Rodman, P.S., 2014. Bipedal and quadrupedal locomotion in chimpanzees. J. Hum. Evol. 66, 64-82.

Prang, C.T., 2015. Calcaneal robusticity in Plio-Pleistocene hominins: Implications for locomotor diversity and phylogeny. J. Hum. Evol. 80, 135-146.

Prang, C.T., 2019. The African ape-like foot of *Ardipithecus ramidus* and its implications for the origin of bipedalism. eLife 8, e44433.

Raichlen, D.A., Gordon, A.D., 2017. Interpretation of footprints from Site S confirms human-like bipedal biomechanics in Laetoli hominins. J. Hum. Evol. 107, 134-138.

Richmond, B.G., Jungers, W.L., 2008. *Orrorin tugenensis* femoral morphology and the evolution of hominin bipedalism. Science 319, 1662-1664.

Roberts, T.J., 2016. Contribution of elastic tissues to the mechanics and energetics of muscle function during movement. J. Exp. Biol. 219, 266-275.

Roberts, T.J., Chen, M.S., Taylor, C.R., 1998. Energetics of bipedal running. II: Limb design and running mechanics. J. Exp. Biol. 201, 2753-2762.

Rodman, P.S., McHenry, H.M., 1980. Bioenergetics and the origin of human bipedalism. Am. J. Phys. Anthropol. 52, 103-106.

Ross, C.F., Lockwood C.A., Fleagle, J., Jungers, W.L., 2002. Adaptation and behavior in the primate fossil record. In: Plavcan J.M., Kay, R.F., Jungers, W.L., van Schaik, C.P., (Eds.), Reconstructing Behavior in the Primate Fossil Record. Kluwer Academic, New York, pp. 1-41.

Royer, T.D., Martin, P.E., 2005. Manipulations of leg mass and moment of inertia: Effects on energy cost of walking. Med. Sci. Sports Exerc. 37, 646-656.

Ruff, C.B., 1995. Biomechanics of the hip and birth in early *Homo*. Am. J. Phys. Anthropol. 98, 527-574.

Sasaki, K., Neptune, R.R., Kautz, S.A., 2009. The relationships between muscle, external, internal and joint mechanical work during normal walking. J. Exp. Biol. 212, 738-744.

Schache, A.G., Brown, N.A.T., Pandy, M.G., 2015. Modulation of work and power by the human lower-limb joints with increasing steady-state locomotion speed. J. Exp. Biol. 218, 2472-2481.

Schmitt, D., 2003. Insights into the evolution of human bipedalism from experimental studies of humans and other primates. J. Exp. Biol. 206, 1437-1448.

Schmitt, D., Larson, S.G., 1995. Heel contact as a function of substrate type and speed in primates. Am. J. Phys. Anthropol. 96, 39-50.

Schmitz, A., Silder, A., Heiderscheit, B., Mahoney, J., Thelen, D.G., 2009. Differences in lower-extremity muscular activation during walking between healthy older and young adults. J. Electromyogr. Kinesiol. 19, 1085-1091.

Schultz, A.H., 1930. The skeleton of the trunks and limbs of higher primates. Hum. Biol. 2, 303-438.

Schultz, A.H., 1961. Vertebral column and thorax. Primatologia 4,1-66.

Simpson, S.W., Levin, N.E., Quade, J., Rodgers, M.J., Semaw, S., 2019. *Ardipithecus ramidus* postcrania from the Gona Project area, Afar Regional State, Ethiopia. J. Hum. Evol. 129, 1-45.

Slider, A., Whittington, B., Heiderscheit, B., Thelen, D.G., 2007. Identification of passive elastic joint moment-angle relationships in the lower extremity. J. Biomech. 40, 2628-2635.

Sockol, M.D., Raichlen, D.A., Pontzer, H., 2007. Chimpanzee locomotor energetics and the origin of human bipedalism. Proc. Natl. Acad. Sci. USA 104, 12265-12269.

Stansfield, B.W., Nicol, A.C., Paul, J.P., Kelly, I.G., Graichen, F., Bergmann, G., 2003a. Direct comparison of calculated hip joint contact forces with those measured using instrumented implants. An evaluation of a three-dimensional mathematical model of the lower limb. J. Biomech. 36, 929-936.

Stansfield, B.W., Hillman, S.J., Hazlewood, M.E., Lawson, A.M., Mann, A.M., Loudon, I.R., Robb, J.E., 2003b. Normalisation of gait data in children. Gait Posture. 17, 81-87.

Stern, J.T., Jr., Susman, R.L., 1981. Electromyography of the gluteal muscles in *Hylobates*, *Pongo*, and *Pan*: Implications for the evolution of hominid bipedality. Am. J. Phys. Anthropol. 55, 153-166.

Stern, J.T., Jr., Larson, S.G., 1993. Electromyographic study of the obturator muscles in non-human primates: Implications for interpreting the obturator externus groove of the femur. J. Hum. Evol. 24, 403-427.

Susman, R.L., 1983. Evolution of the human foot: Evidence from Plio-Pleistocene hominids. Foot Ankle 3, 365-376.

Susman, R.L., Stern, J.T., Jr., Jungers, W.L., 1984. Arboreality and bipedality in the Hadar hominids. Folia Primatol. 43, 113-156.

Sutherland, D., 1997. The development of mature gait. Gait Posture. 6, 163-170.

Takanashi, K.Z., Worster, K., Bruening, D.A., 2017. Energy neutral: The human foot and ankle subsections combine to produce near zero net mechanical work during walking. Sci. Rep. 7, 15404.

Thorpe, S.K.S., Crompton, R.H., Gunther, M.M., Ker, R.F., Alexander, R.McN., 1999. Dimensions and moment arms of the hind- and forelimb muscles of common chimpanzees (*Pan troglodytes*). Am. J. Phys. Anthropol. 110, 179-199.

Umberger, B.R., Rubenson, J., 2011. Understanding muscle energetics in locomotion: New modeling and experimental approaches. Exerc. Sports Sci. Rev. 39, 59-67.

Vereecke, E., D'Août, K., De Clercq, D., van Elsacker, L., Aerts, P., 2003. Dynamic plantar pressure distribution during terrestrial locomotion of bonobos (*Pan paniscus*). Am. J. Phys. Anthropol. 120, 373-383.

Vrahas, M.S., Brand, R.A., Brown, T.D., Andrews, J.G., 1990. Contribution of passive tissues to the intersegmental moments at the hip. J. Biomech. 23, 357–62.

Ward, C.V., 1993. Torso morphology and locomotion in *Proconsul nyanzae*. Am. J. Phys. Anthropol. 92, 291-328.

Ward, C.V., Hammond, A.S., Plavcan, J.M., Begun, D.R., 2019. A late Miocene hominoid partial pelvis from Hungary. J. Hum. Evol. 136, 102645.

Warrener, A.G., 2017. Hominin hip biomechanics: Changing perspectives. Anat. Rec. 300, 932-945.

Webber, J.T., Raichlen, D.A., 2016. The role of plantigrady and heel-strike in the mechanics and energetics of human walking with implications for the evolution of the human foot. J. Exp. Biol. 219, 3729-3737.

Whittington, B., Slider, A., Heiderscheit, B., Thelen, D.G., 2008. The contribution of passive-elastic mechanisms to lower extremity joint kinetics during human walking. Gait Posture 27, 628-634.

Winter, D.A, Yack, H.J., 1987. EMG profiles during normal human walking: Stride-to-stride and inter-subject variability. Electro. Clinical Neurophys. 67, 402-411.

Woledge, R.C., Curtin, N.A., Homsher, E., 1985. Energetic Aspects of Muscle Contraction. Academic Press, London.

Yoon, Y.S., Mansour, J.M., 1982. The passive elastic moment at the hip. J. Biomech. 15, 905–10.

Yamazaki, N., Ishida, H., Kimura, T., Okada, M., 1979. Biomechanical analysis of primate bipedal walking by computer simulation. J. Hum. Evol. 8, 337-349.

Yamazaki, N., 1985 Primate bipedal walking: Computer simulation. In: Kondo, S. (Ed.), Primate Morphophysiology, Locomotor Analyses, and Human Bipedalism. U Tokyo Press, Tokyo, pp. 105-130.

Zelik, K.E., Kuo, A.D., 2010. Human walking isn't all hard work: Evidence of soft tissue contributions to energy dissipation and return. J. Exp. Biol. 213, 4257-4264.

Zelik, K.E., Takahashi, K.Z., Sawicki GS. 2015. Six degree-of-freedom analysis of hip, knee, ankle and foot provides updated understanding of biomechanical work during human walking. J. Exp. Biol. 218, 876-886.

Zelik, K.E., Franz, J.R. 2017. It's positive to be negative: Achilles tendon work loops during human locomotion. PLoS One. 12, e0179976.

1

2 Zelik, K.E., Honert, E.C., 2018. Ankle and foot power in gait analysis: Implications for
3   science, technology and clinical assessment. J. Biomech. 75, 1-12.

4

5 Zihlman, A., Bolter, D., Boesch, C., 2004. Wild chimpanzee dentition and its
6   implications for assessing life history in immature hominin fossils. Proc. Natl.
7   Acad. Sci. USA 101, 10541-10543.

8

1 **Figure legends**
2
3 **Figure 1.** A full bipedal walking stride. A full stride includes both stance and swing
4 phases. The stance phase is divided among the first double support (double support 1),
5 single support, and the second double-support (double support 2) periods. In the first
6 double-support period the right hind limb is the leading limb, while in the second double-
7 support period the right hind limb is the trailing limb. The green arrow shows the
8 direction and relative magnitude of the resultant ground reaction force under each foot
9 over a full stride.

10

11 **Figure 2.** The vertical (A–B), anterior-posterior (C–D) and medio-lateral (E–F) ground
12 reaction forces over a walking step (mean ± s.d.) for the three chimpanzees (column 1) as
13 well as chimpanzees (solid blue line) and humans (dashed black line) as groups (column
14 2). Each step begins at heel strike (i.e., foot touchdown) and ends at toe off of the same
15 foot. Broken vertical lines show the average step event times for the chimpanzees,
16 representing contralateral limb toe off (H = 21%, C = 23%) and the contralateral limb
17 heel strike (H = 81%, C = 77%), which define the double-support and single support
18 periods of a step.

19

20 **Figure 3.** The hip flexion-extension moment (A), abduction-adduction moment (B),
21 internal-external rotation (C), knee flexion-extension moment (D) and ankle plantar
22 flexion-dorsiflexion moment (E) over a walking stride (mean ± s.d.) for chimpanzees
23 (solid blue line) and humans (dashed black line). Moments are in dimensionless units.
24 Each stride begins and ends at ipsilateral 'heel strike' (i.e., foot touchdown). All vertical
25 lines show the average stride event times for the chimpanzees, which were similar among
26 the species. The broken vertical lines represent contralateral limb toe-off (H = 13%, C =
27 14%) and contralateral limb 'heel strike' (H = 51%, C = 48%), which define the double-
28 support and single support periods of a stride; the solid vertical line represents ipsilateral
29 toe off (H = 63%, C = 62%), which defines the start of the swing phase.

30

31 **Figure 4.** The 3-D hip power (A), knee power (B), and ankle power output (C) over a
32 walking stride (mean ± s.d.) for humans (dashed black line) and chimpanzees (solid blue

1   line). All vertical lines show the average stride event times for the chimpanzees, which

2   were similar among the species. The broken vertical lines represent contralateral limb

3   toe-off (H = 13%, C = 14%) and contralateral limb 'heel strike' (H = 51%, C = 48%),

4   which define the double-support and single support periods of a stride; the solid vertical

5   line represents ipsilateral toe off (H = 63%, C = 62%), which defines the start of the

6   swing phase. Powers are in dimensionless units.

7

8   **Figure 5.** The stance phase positive joint work (A) and power (B) output in the first

9   double support (DS1), single support (SS) and second double-support (DS2) period of a

10   walking stride for humans (black) and chimpanzees (red) (mean ± s.d.). The relative

11   contributions of the ankle elastic work and power ('ankle elastic') and muscle fiber work

12   and power ('muscle fiber') to the total limb work and power output in the human DS2

13   period is shown.

14

15   **Figure 6.** Total positive limb work (A) and average positive limb power (B) used to

16   swing the limb during walking in humans (black) and chimpanzees (red; mean ± s.d.).

17

18   **Figure 7.** Total positive limb work (A) and average positive limb power (B) over a full

19   walking stride in humans (black) and chimpanzees (red; mean ± s.d.). The human total

20   lower limb work and power is due to contributions from both elastic mechanisms at the

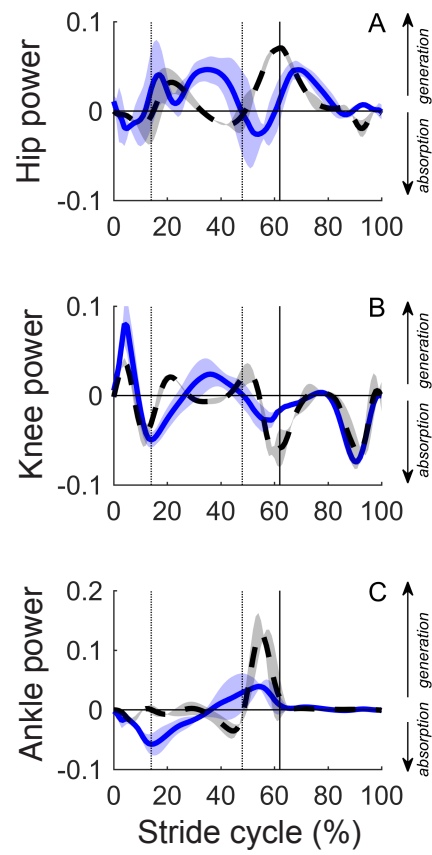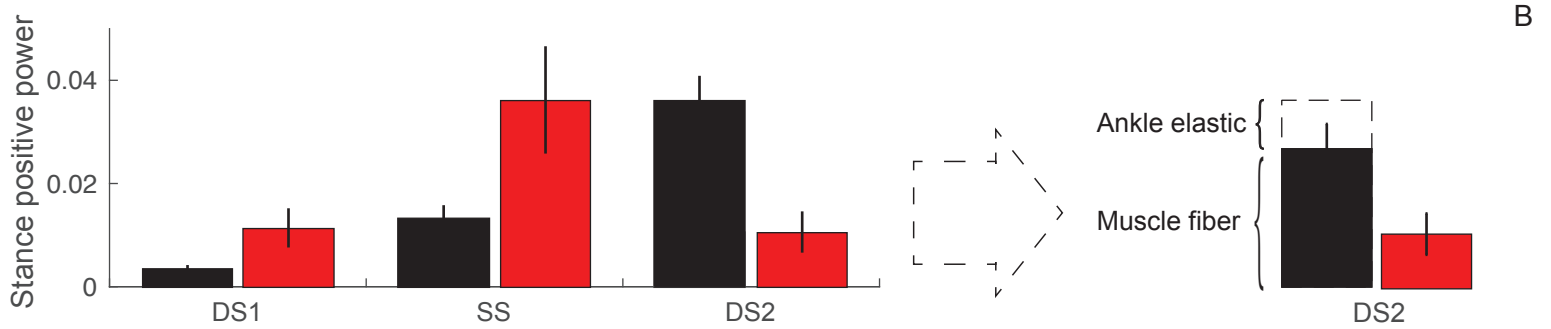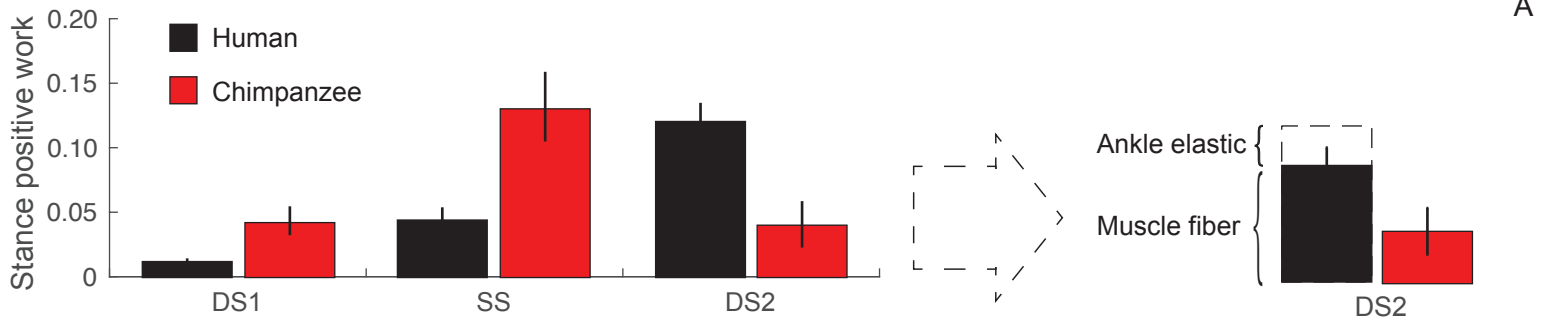21   hip and ankle ('elastic') as well as muscle fibers ('muscle fiber').

22

23   **Figure 8.** The distribution of positive mechanical work (A) and negative mechanical

24   work among the limb joints (B) during stance and swing in humans (column 1) and
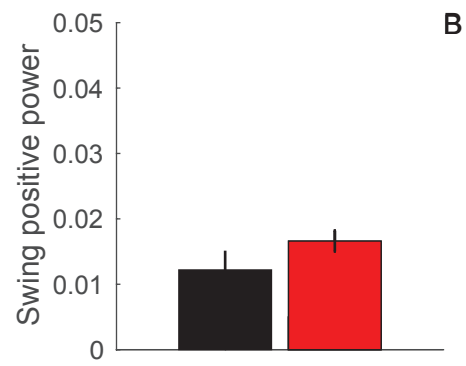
25   chimpanzees (column 2).

Stance phase
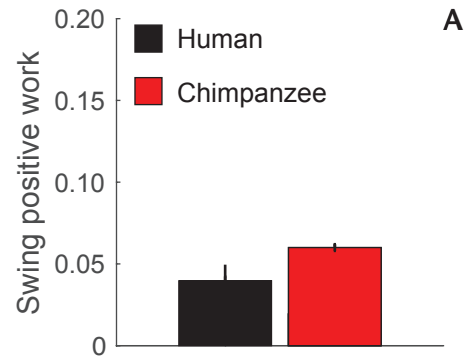
Swing phase

Double support 1
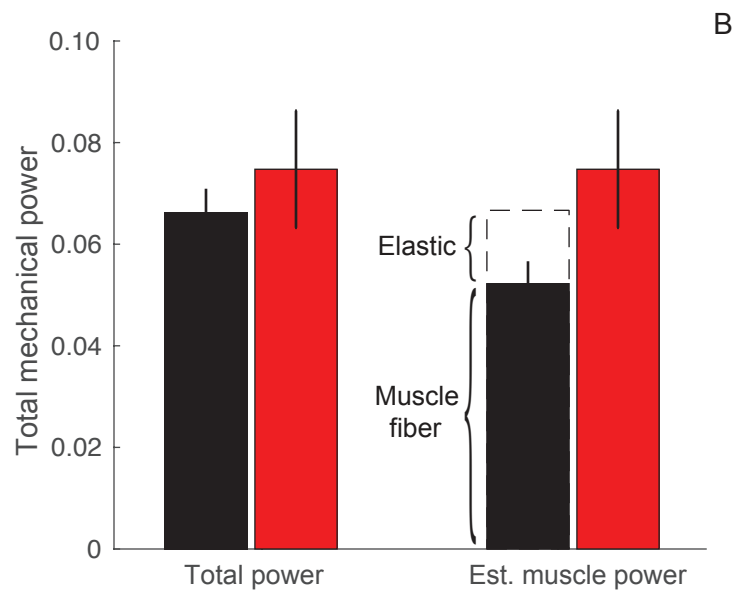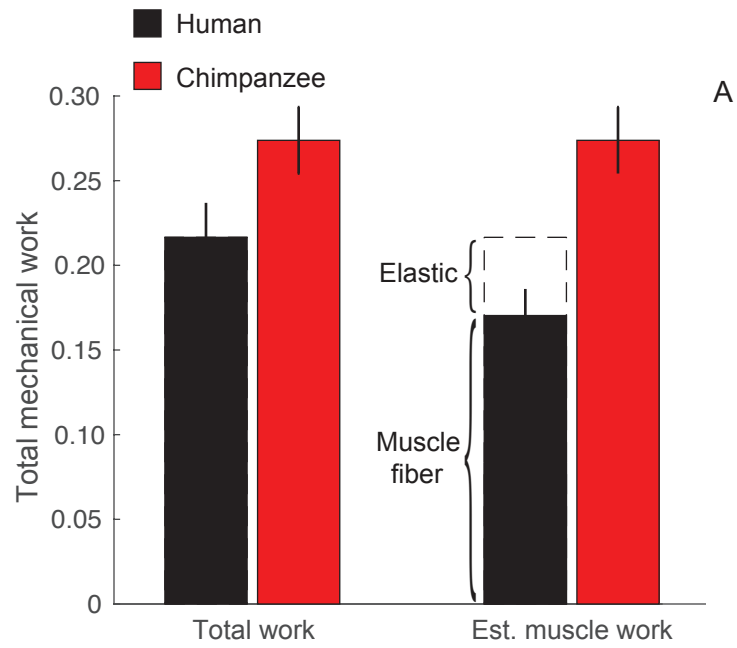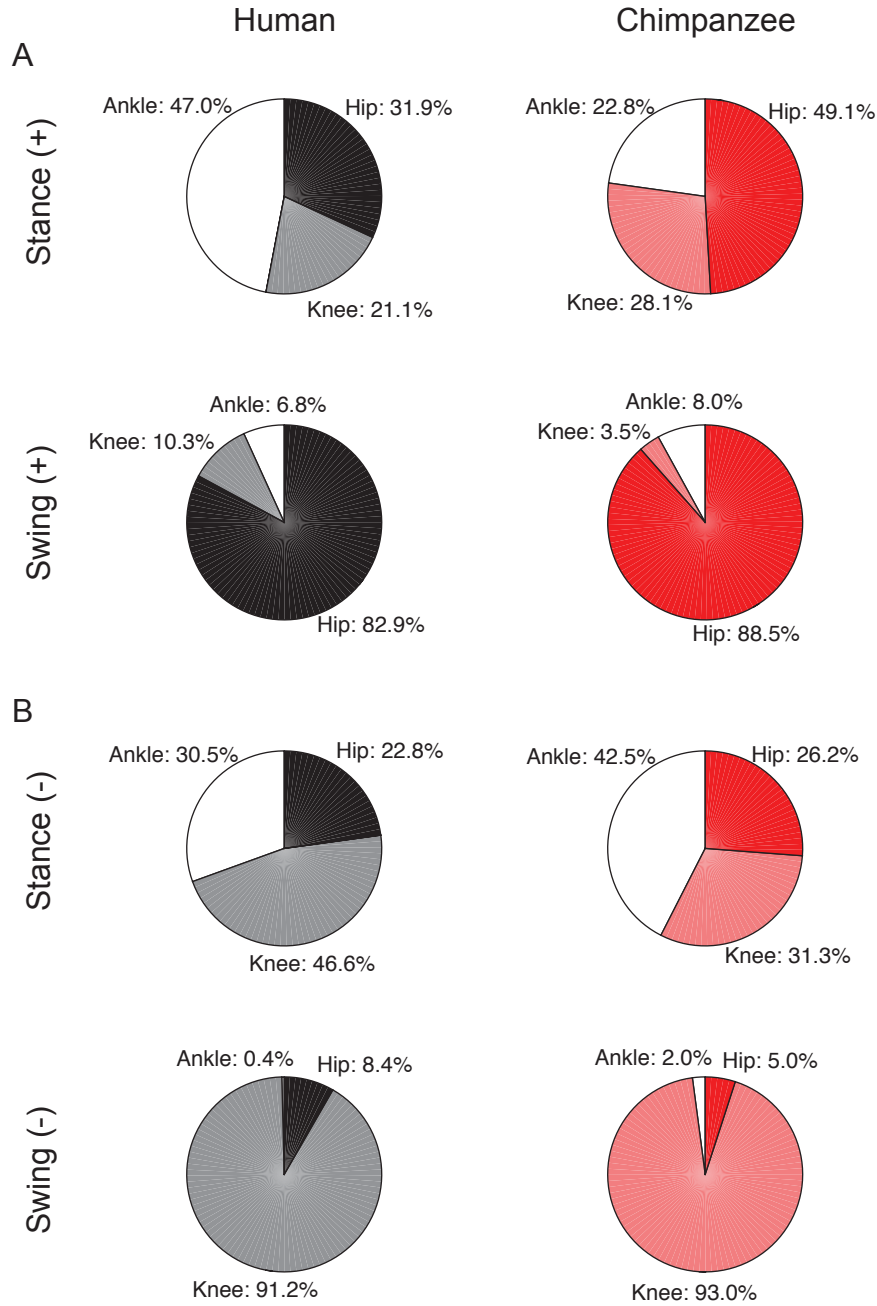
Single support

Double support 2
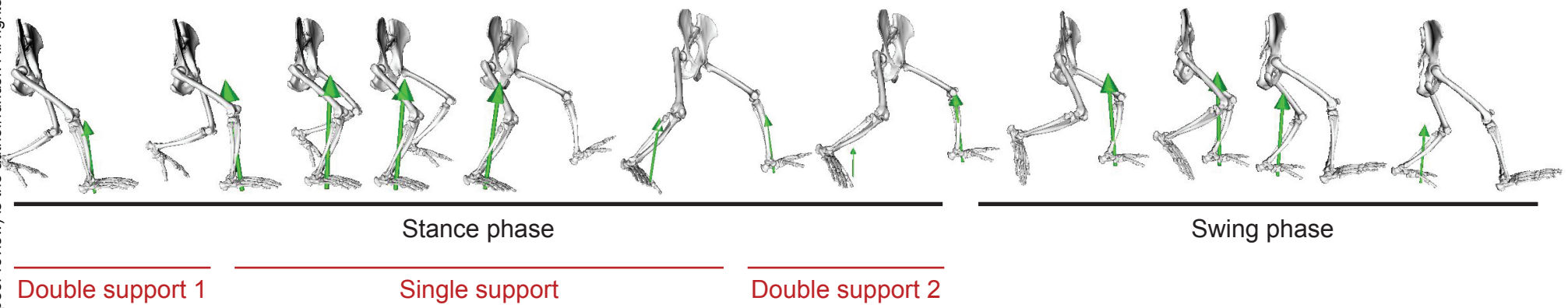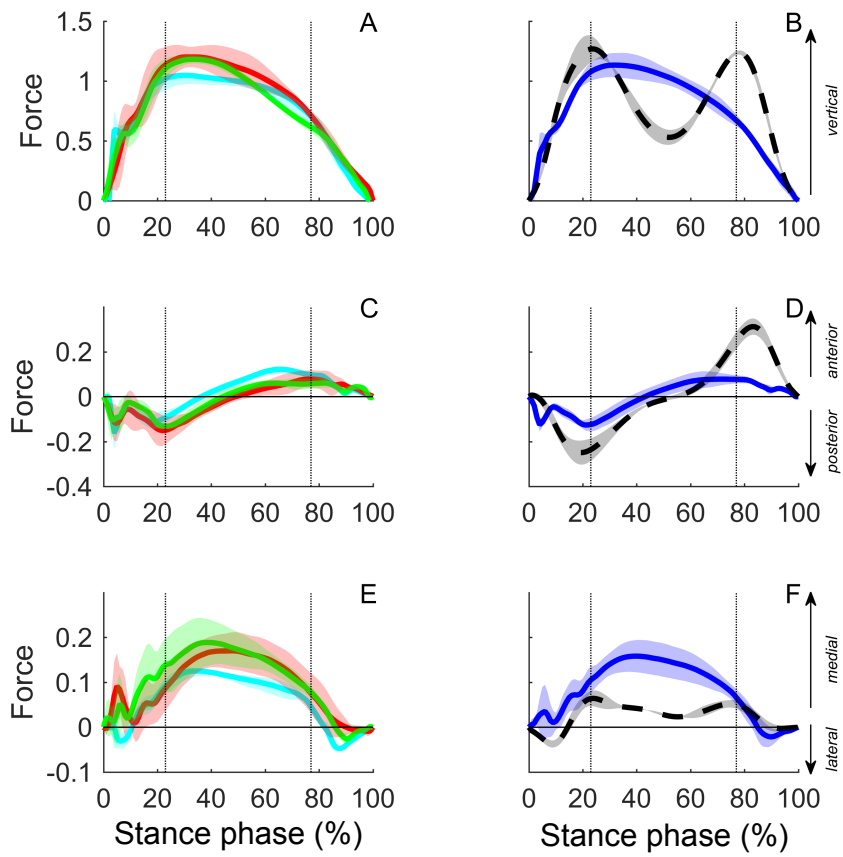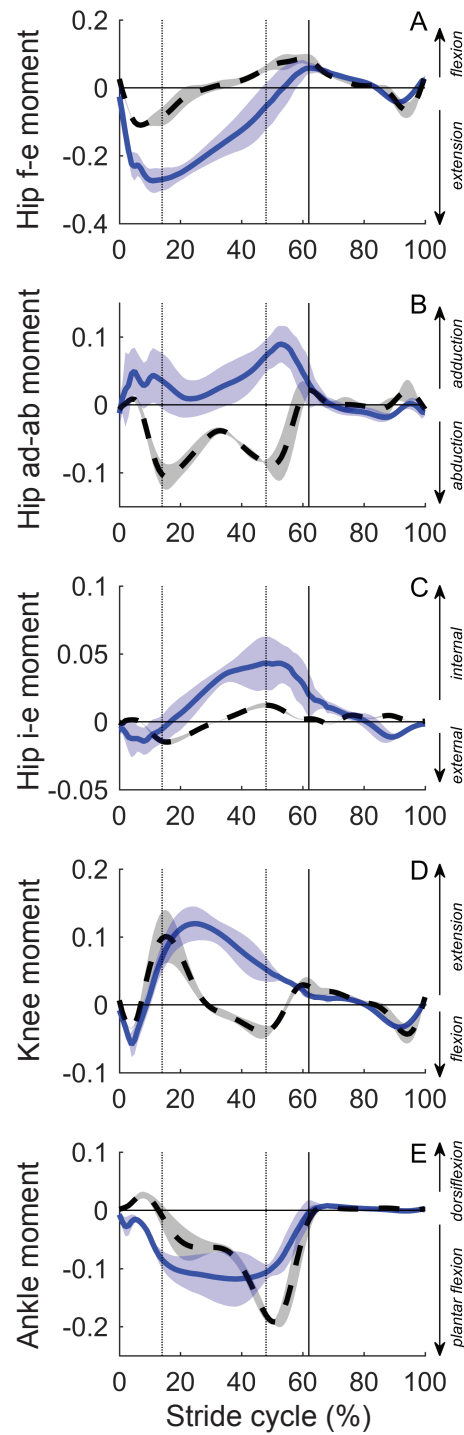
Table 1

Spatiotemporal gait parameters in human and chimpanzee bipedal walking. Human data are matched to the chimpanzee data in dimensionless (i.e., relative-speed match) form (mean ± s.d.).

	v[a] (m s^{-1})	v[b]	Fr[c]	Stance time (s)	Swing time (s)	Stride length (m)	Stride frequency (Hz)	Duty factor
Humans	1.66 ± 0.06	0.56 ± 0.01	0.31 ± 0.02	0.64 ± 0.02	0.36 ± 0.04	1.69 ± 0.05	1.00 ± 0.05	0.64 ± 0.02
Chimpanzees	1.09 ± 0.10	0.56 ± 0.06	0.31 ± 0.06	0.45 ± 0.09	0.27 ± 0.03	0.78 ± 0.07	1.43 ± 0.23	0.62 ± 0.03

[a] Dimensional velocity.
[b] Dimensionless velocity.
[c] Froude number.

Table 2

Adjusted coefficient of multiple correlation (CMC) of ground reaction forces (F_y, F_x, F_z).

	$F_{y, vert}$	$F_{x, ant-post}$	$F_{z, med-lat}$
Humans[a]	0.994 ± 0.003	0.996 ± 0.001	0.965 ± 0.017
Among humans[b]	0.958 ± 0.018	0.972 ± 0.007	0.916 ± 0.038
Chimpanzees[a]	0.972 ± 0.021	0.911 ± 0.054	0.884 ± 0.074
Among chimpanzees[b]	0.962 ± 0.016	0.883 ± 0.031	0.847 ± 0.012

Human data are matched to the chimpanzee data in dimensionless (i.e., relative-speed match) form (mean ± s.d.). CMC mean ± s.d. for 4 trials per subject, 3 subjects. The y, x, z components of the ground reaction forces are vertical (vert), anterior-posterior (ant-post) and medial-lateral (med-lat).

[a] Correlations between strides within subjects.

[b] Correlations between subjects.

Table 3

Peak joint moments in bipedal chimpanzees and humans in dimensionless units. Human data are matched to the chimpanzee data in dimensionless (i.e., relative-speed match) form (mean ± s.d.).

	Hip			Knee	Ankle
	Flexion-extension	Adduction-abduction	Internal-external rotation	Flexion-extension	Plantar flexion-dorsiflexion
Humans	-0.112 ± 0.006 (ext.)	-0.106 ± 0.019 (abd.)	0.025 ± 0.003 (int.)	0.102 ± 0.038 (ext.)	-0.196 ± 0.002 (plantar.)
Chimpanzees	-0.274 ± 0.036 (ext.)	0.093 ± 0.029 (add.)	-0.047 ± 0.016 (ext.)	0.122 ± 0.024 (ext.)	-0.131 ± 0.037 (plantar.)

The direction of the peak joint moment is given as flexion (flex.), extension (ext.), abduction (abd.), adduction (add.), internal rotation (int.), external rotation (ext.), plantar flexion (plantar.) or dorsiflexion (dorsi.).

Table 4

Peak joint power in bipedal chimpanzees and humans at matched dimensionless speeds in dimensionless units. Human data are matched to the chimpanzee data in dimensionless (i.e., relative-speed match) form (mean ± s.d.).

	Hip power		Knee power		Ankle power	
	+	−	+	−	+	−
Humans	0.071 ± 0.010	−0.031 ± 0.002	0.038 ± 0.004	−0.078 ± 0.005	0.145 ± 0.037	−0.034 ± 0.011
Chimpanzees	0.067 ± 0.016	−0.050 ± 0.016	0.083 ± 0.027	−0.076 ± 0.004	0.052 ± 0.014	−0.059 ± 0.018